

Activation State of the Supramammillary Nucleus Regulates Body Composition and Peripheral Fuel Metabolism

Yahong Zhang,* Carl Stoelzel Michael Ezrokhi, Tsung-Huang Tsai and Anthony H. Cincotta*

VeroScience LLC, Tiverton, RI 02878, United States

Abstract—Whole body fuel metabolism and energy balance are controlled by an interactive brain neuronal circuitry involving multiple brain centers regulating cognition, circadian rhythms, reward, feeding and peripheral biochemical metabolism. The hypothalamic supramammillary nucleus (SuMN) comprises an integral node having connections with these metabolically relevant centers, and thus could be a key central coordination center for regulating peripheral energy balance. This study investigated the effect of chronically diminishing or increasing SuMN neuronal activity on body composition and peripheral fuel metabolism. The influence of neuronal activity level at the SuMN area on peripheral metabolism was investigated via chronic (2–4 week) direct SuMN treatment with agents that inhibit neuronal activity (GABA_A receptor agonist [Muscimol] and AMPA plus NMDA glutamate receptor antagonists [CNQX plus dAP5, respectively]) in high fat fed animals refractory to the obesogenic effects of high fat diet. Such treatment reduced SuMN neuronal activity and induced metabolic syndrome, and likewise did so in animals fed low fat diet including inducement of glucose intolerance, insulin resistance, hyperinsulinemia, hyperleptinemia, and increased body weight gain and fat mass coupled with both increased food consumption and feed efficiency. Consistent with these results, circadian-timed activation of neuronal activity at the SuMN area with daily local infusion of glutamate receptor agonists, AMPA or NMDA at the natural daily peak of SuMN neuronal activity improved insulin resistance and obesity in high fat diet-induced insulin resistant animals. These studies are the first of their kind to identify the SuMN area as a novel brain locus that regulates peripheral fuel metabolism. © 2021 VeroScience LLC. Published by Elsevier Ltd on behalf of IBRO. This is an open access article under the CC BY-NC-ND license (<http://creativecommons.org/licenses/by-nc-nd/4.0/>).

Key words: insulin resistance, glucose intolerance, obesity, metabolic syndrome, feeding.

INTRODUCTION

Central nervous system (CNS) regulation of whole body fuel metabolism involves a complex interaction between brain cognitive, executive and reward centers (e.g., the prefrontal cortex, hippocampus, amygdala, and mesolimbic system) regulating cognition, learning/memory, reward assessment, arousal, motivation, reward seeking behavior (Berridge et al., 2010; Egcioglu et al., 2011; Ferrario et al., 2016; Johnson, 2013) and brain metabolic homeostasis centers in the hypothalamus and brain stem regulating feeding and peripheral biochemical metabolism (Lutz, 2012; Schwartz et al., 2000; Seoane-Collazo et al., 2015; Timper and Bruning, 2017; Travagli et al., 2006; Uyama et al., 2004). How functions within these multiple brain centers are coordinated and integrated to establish a particular metabolic status (i.e., lean, insulin sensitive vs obese, insulin resistant state) is not completely understood. However, evidence suggests that the

supramammillary nucleus (SuMN) in the posterior hypothalamus could be one of the key CNS centers for integrating feeding, feeding-related behaviors and feeding-independent peripheral metabolic functions to thereby control body energy balance and metabolism.

The SuMN is a small elongated nucleus composed of medial and lateral parts overlying the mammillary body in the posterior hypothalamus and sits anterior to the ventral tegmental area (VTA). Although small in size, this nucleus consisting of a heterogeneous population of neurons (e.g., glutamatergic, GABAergic, neuropeptidergic and dopaminergic) has marked influences on a broad spectrum of brain areas that modulate cognition, ingestive behavior, reward and energy metabolism including the prefrontal cortex, hippocampus, mesolimbic system, hypothalamus and raphe nuclei (Ikemoto, 2010; Pan and McNaughton, 2004). The SuMN regulates hippocampal theta rhythm (Pan and McNaughton, 2002; Ruan et al., 2017; Vertes, 2015) which in turn, through massive projections to the lateral septum-hypothalamus pathway, modulates ingestive behaviors (Risold and Swanson, 1996; Tsanov, 2018). The SuMN also modulates the VTA-nucleus accumbens

*Corresponding author.

E-mail addresses: Yahong_Zhang@veroscience.com (Y. Zhang), Anthony_Cincotta@veroscience.com (A. H. Cincotta).

dopamine reward systems via relay nuclei to modulate reward interpretation and motivated behavior (Ikemoto, 2010). Moreover, the SuMN connects with several brain arousal promoting regions including the lateral hypothalamus, the serotonergic raphe nuclei, noradrenergic locus coeruleus and the cholinergic lateral dorsal tegmental nucleus (Gonzalo-Ruiz et al., 1999; Hayakawa et al., 1993; Ikemoto, 2010; Pan and McNaughton, 2004; Swanson, 1982; Vertes, 1992), and is implicated in the regulation of arousal and wakefulness (Pedersen et al., 2017; Stagkourakis et al., 2018). Historically, its role has thus far been most thoroughly defined as integration and modulation of cognition and emotional aspects of goal-oriented behaviors and all these functions need to be summoned in decision making and executing ingestive behaviors.

In addition to its role in modulating behavioral activities, very recent studies have suggested a potential role for the SuMN in the regulation of feeding and feeding-independent fuel metabolism. The SuMN neuronal activity exhibits a circadian day-night activity pattern in synchrony with that of locomotor activity in animals (Castillo-Ruiz et al., 2013). It has been demonstrated that the dopamine neurons at the medial SuMN constitute a major source of dopaminergic input to the suprachiasmatic nucleus (SCN) area where circadian dopamine input activity exerts strong control over peripheral fuel metabolism. The circadian peak in dopaminergic activity at the SCN area is functional in maintaining insulin sensitivity (Luo et al., 2018). Additionally, the SuMN has distinct connections with other hypothalamic metabolic regulatory neuronal centers (e.g., the ventromedial hypothalamic nucleus [VMH]) (Plaisier et al., 2020) and is capable of sensing and responding to feeding-regulatory molecules (e.g., GLP-1 and GLP-1—estrogen conjugate induced acute inhibition of feeding; ghrelin induced acute feeding) (Le May et al., 2019; Lopez-Ferreras et al., 2019; Vogel et al., 2016; Leranath et al., 1999b). Consequently, the SuMN may very well function as an integration/coordination center of circadian feeding behavior and circadian metabolic processes in the peripheral tissues (e.g., liver, adipose, muscle). Nevertheless, the impact of chronic alterations in SuMN circadian neuronal activity, either inhibited over the 24-h day or stimulated at its natural circadian peak activity time, on peripheral fuel metabolism, body composition, or feed efficiency has never been investigated and no known role for SuMN in metabolic control of either glucose tolerance or insulin sensitivity has been delineated.

The SuMN neuronal activity is regulated by dynamic interactions between stimulatory glutamate and inhibitory GABA input signaling emanating from multiple brain regions (Gonzalo-Ruiz et al., 1999; Kiss et al., 2002; Leranath et al., 1999a). Such GABA and glutamate signaling, including their moment-to-moment interactions, each via very different cellular signal transduction mechanisms, could be translated by homogenous or heterogeneous SuMN neurons into informative output signals to mobilize different or overlapping neuronal circuits regulating multiple aspects of peripheral energy metabolism. Notable differences exist between the medial and lateral

parts of the SuMN in their neuronal chemical contents and specificity of neuronal connections (Pan and McNaughton, 2004; Soussi et al., 2010); in particular the SuMN-SCN clock-projecting dopamine neurons that may regulate its control of metabolism are located exclusively in the medial SuMN (Luo et al., 2018; Shepard et al., 1988; Swanson, 1982). The present study therefore was designed to investigate the influence of direct (a) sustained pharmacological attenuation of neuronal activities at the medial SuMN area via stimulating GABA signaling with GABA_A receptor agonist or via inhibiting glutamate stimulatory signaling with AMPA/NMDA receptor antagonists and their combinations, as well as (b) circadian-timed stimulation (with AMPA or NMDA) of neuronal activities at the medial SuMN area (at the time of day of its natural daily peak neuronal activity) respectively on feeding, body composition, glucose tolerance, insulin sensitivity, and other aspects of peripheral metabolism in animals fed regular chow and those resistant or sensitive to the obesogenic effects of a high fat diet.

EXPERIMENTAL PROCEDURES

Animals

Female Sprague-Dawley (SD) rats (10–12 weeks of age) (Taconic Biosciences, Hudson, NY) were housed individually in a temperature- and humidity-controlled room under 14-h light photoperiod (14 h Light and 10 h Dark, 14:10 LD). Rats were allowed to adapt to the animal care facility for 1–2 weeks before the initiation of experiments. To avoid the confounder of age-induced insulin resistance upon the background metabolic status of the study animals during the study period, female rats were used inasmuch as they maintain a steady state of insulin sensitivity for a long period of their life time versus male rats of this strain that develop insulin resistance progressively from an early age (Cincotta et al., 1993; Goodman et al., 1983). For the similar reason, animals were held on a long 14-h daily photoperiod to avoid the confounder of a short ≤ 12 -h light photoperiod-induced insulin resistance upon the background metabolic status of the study animals during the study period (Meier and Cincotta, 1996). Depending on the individual experimental design, rats were fed either a high fat diet (HFD) (60% of calories/gram from fat, Research Diets Inc, d12492) or regular chow (18% of calories/gram from fat, Envigo Teklad 2018) and water *ad libitum*. All animal experiments were conducted in accordance with the National Institutes of Health Guide for the Care and Use of Experimental Animals and with the protocols approved by the Institutional Animal Care and Use Committee of VeroScience, LLC.

Drugs

The GABA_A receptor agonist Muscimol (5-Aminomethyl-3-hydroxyisoxazole, cat# 0289), the AMPA receptor antagonist CNQX disodium salt (6-Cyano-7-nitroquinoxaline-2,3-dione disodium, cat# 1045) and the NMDA receptor antagonist dAP5 (D-(–)-2-Amino-5-phosphono pentanoic acid, cat# 0106) were purchased from R&D

systems, Inc. (Minneapolis, MN). A neuronal inhibitory Dual Cocktail (DC) was prepared by mixing Muscimol and CNQX in saline. A neuronal inhibitory Triple Cocktail (TC) was prepared by mixing Muscimol, CNQX and dAP5 in saline and titrated with 1 N NaOH to pH7 due to the acidity of dAP5. The continuous infusion doses of Muscimol (0.6 mM/0.25 μ l/h, 3.6 nmol/day) (Gliddon et al., 2005), CNQX (0.3 mM/0.25 μ l/h, 1.8 nmol/day) (Broadbent et al., 2010; Shabat-Simon et al., 2008) and dAP5 (20 mM/0.25 μ l/h, 120 nmol/day) (Davis et al., 1992; Morris et al., 2013) were chosen based on such previous publications and test results in our own hands (see below). Similar metabolic effects on insulin sensitivity, body weight/fat and food consumption were observed when a lower dose of dAP5 (2 mM, 12 nmol/day) was used in the TC (see below Study 6). The glutamate NMDA receptor agonist NMDA (N-methyl-D-aspartic acid) (cat# 0114, Tocris Bioscience) and its co-agonist D-serine (cat# 0226, Tocris Bioscience), and the AMPA receptor agonist (s)-AMPA (α -amino-3-hydroxy-5-methyl-4-isoxazolepropionic acid) (cat# A0326, Sigma) were prepared in artificial cerebral spinal fluid fresh daily before use. The effective doses of AMPA (30 pmol, 0.5 μ l) and NMDA/D-serine (250 pmol/250 pmol, 0.5 μ l) for circadian-timed daily infusion were chosen to sufficiently activate neuronal activity based on results from several similar previous studies (Ikemoto, 2004; Ikemoto et al., 2004; Kretschmer, 1999; Stalnaker and Berridge, 2003) and verified in our own hands and are much lower than the reported neuronal toxicity doses for these agents (Kimbrow et al., 2000; Rambousek et al., 2016).

Surgery, cannula placement and drug infusion procedure

Animals were anesthetized with ketamine/xylazine (80 mg/12 mg/kg, ip) and secured on a stereotaxic apparatus. For continuous local infusion at the medial SuMN, a cannula (30/21GA, Plastics One) with an arm connected to a mini-osmotic pump (Alzet 2004, 0.25 μ l/h) filled with vehicle, dual cocktail (Muscimol/CNQX, 3.6/1.8 nmol/day) or triple cocktail (Muscimol/CNQX/dAP5, 3.6/1.8/120 nmol/day) was implanted at the medial SuMN (4.55 mm posterior to Bregma; 0.2 mm from midline; 8.4 mm ventral to Bregma). The armed cannula was firmly anchored to the skull with three stainless-steel screws and cemented in position with dental acrylic cement. The mini-osmotic pumps were replaced with new ones filled with freshly prepared cocktail solutions every 2 weeks. For circadian-timed daily local infusion at the medial SuMN (see Study 7 below), a guide cannula (26GA, Plastics One) with its stylet was implanted at the medial SuMN according to the following coordinates: 4.55 mm posterior from Bregma, 0.2 mm from midline, 7.4 mm ventral to Bregma and secured to the skull with dental acrylic cement. Animals were allowed to recover from surgery for 3 days before starting daily infusions. Vehicle, AMPA (30 pmol) or NMDA/D-serine (250/250 pmol) was infused at the medial SuMN (0.5 μ l) over one minute via an injector with 1 mm protrusion lowered to the medial SuMN through a chronically implanted guide cannula.

After infusion, the injector was left in place for an additional minute before slow withdrawal. At the end of the experiment, the cannula placement was verified histologically on coronal brain sections at the level of the SuMN and the data collected from the animals with correct placement were used for statistical analyses.

Study 1: Verification of cannula placement and assessment of the time-dependent diffusion/distribution of infused receptor ligands within the medial SuMN and surrounding area

The cannula placement at the medial SuMN was examined histologically by hematoxylin staining on coronal brain sections at the level of the SuMN. Black nigrosin was used for assessment of acute distribution of infused receptor ligand at the medial SuMN. Nigrosin has a molecular weight of 453.5, approximately that of the neurotransmitter receptor ligands employed in this study. Nigrosin was prepared in saline at molar concentrations either comparable to (0.6 mM), 6 times greater (3 mM) or 20 times greater (10 mM) than the highest molar concentration of the acutely infused drugs used in the experiments (e.g., NMDA at 0.5 mM and microinfused [0.5 μ l] at the medial SuMN). The brains (from 4 rats for each dose) were collected at 3 h post-microinfusion, quickly frozen on dry ice and sectioned using a cryostat at -20°C . The black nigrosin deposit at the medial SuMN was examined under a dissection microscope (4 \times magnification) and photographed. Next, the tissue distribution of receptor ligands (e.g., muscimol) following their continuous infusion through an osmotic pump for a period from 2 to 4 weeks was evaluated using fluorescent muscimol (Muscimol-TMR-X, Molecular Probes M23400) which is as functional as unlabeled muscimol (Allen et al., 2008). Muscimol-TMR-X has a molecular weight of 607.46, generally comparable to unlabeled muscimol (MW = 114.1). Muscimol-TMR-X is stable and will not dissociate into its constituent parts in solution and TMR-X portion is highly lipophilic (Molecular Probes, Technical Support, Carlsbad, CA). Muscimol-TMR-X was prepared at the same concentration of muscimol (0.6 mM) used in the experiments and similarly microinfused at the medial SuMN through an implanted osmotic pump (Alzet 2004, 0.25 μ l/h). The rats (5 rats at each time point) were subsequently sacrificed after 2 and 4 weeks following such continuous infusion and the brains were collected following transcardiac perfusion with 4% paraformaldehyde, sectioned at 35 microns, and examined for fluorescence via microscopy. Another group of rats was similarly infused with nigrosin (0.6 mM) for 2–4 weeks and examined for SuMN staining under light microscopy.

Study 2: Verification of glutamate and GABA_A receptor ligands and their combinations (inhibitory dual and triple cocktails) in modulation of the activation state of the medial SuMN region

After 2 weeks of habituation to the animal care facility (14 h light photoperiod), SD rats (14 weeks old, BW = 277 ± 2.3 g) were separated into 2 experiments

(Exp 2A and Exp 2B) and maintained on regular chow during the study period. In Exp 2A, multiunit firing activity at the medial SuMN area in response to acute iontophoretic applications of either (a) stimulatory ligands (glutamate, AMPA, or NMDA/D-serine) or (b) inhibitory ligands (Muscimol, CNQX, or dAP5) following stimulatory ligand presentation were studied. Inhibitory ligand testing included testing of both dual and triple cocktails. In Exp 2B, rats received SuMN infusion of triple cocktail (Muscimol/CNQX/dAP5, 0.6 mM/0.3 mM/2 mM, 0.25 μ l/h, 3.6/1.8/12 nmol/day) for 10–14 days before multi-unit firing activity at the medial SuMN area in response to acute glutamate (70 mM) infusion with or without subsequent acute triple cocktail infusion (Muscimol/CNQX/dAP5, 0.6 mM/0.3 mM/2 mM), respectively was studied.

Surgical preparation and recording. In Exp 2A, rats were anesthetized with ketamine/xylazine (100 mg/10 mg/kg, ip) and mounted into a stereotaxic frame. Body temperature was maintained at 37 °C via a heating pad. A midline incision was made to expose the underlying skull. A small (1.5 mm in diameter) craniotomy was made over the left or right hemisphere, to allow access to the medial SuMN (centered 4.55 mm posterior to Bregma and 0.2 mm lateral of the midline), and a second 1 mm craniotomy was made 4–5 mm posterior of Bregma and 2–4 mm lateral of the midline in the contralateral hemisphere where a silver wire was placed above the dura to serve as ground/reference. Dura was then removed and a three-barrel micro-pipette with central barrel filled with a low impedance carbon fiber recording electrode (Carbostar, Kation Scientific, Minnesota) was implanted into the SuMN (8.4 mm ventral to Bregma). Separate drug administration pipettes were pre-filled with de-ionized water containing one or more of the test compounds (glutamate 250 mM, AMPA 50 mM, CNQX 50 mM, Muscimol 50 mM, dAP5 50 mM, NMDA 50 mM/D-serine 50 mM) and given a holding current of + 10nA for anions or –20nA for cations. Extracellular voltages were recorded for one second, followed by a brief 2 s iontophoretic injection of test compound (injection currents ~ –40nA for anions, and ~+20 nA for cations). This cycle was repeated at a rate of ~ 0.2 Hz for at least 100 cycles. In the case of testing the responsiveness to presumptively inhibitory compounds (Muscimol, CNQX or dAP5), baseline activity was increased through the continuous iontophoretic injection of an excitatory test compound (glutamate, AMPA, or NMDA/D-serine, respectively), with glutamate being used in the cases of dual and triple inhibitory cocktail testing.

In Exp 2B, rats were similarly anesthetized, and craniotomy was performed in the same way as described above in Exp 2A. To chronically infuse inhibitory triple cocktail at the medial SuMN area, a

double barrel stainless steel guide cannula (21 and 26 gauge) was implanted 3 mm above the medial SuMN. A 33 gauge internal cannula was put inside the 21 gauge external cannula, terminating 3 mm below the external, so that the tip would be positioned at 8.4 mm ventral to Bregma, and this cannula was connected to an chronically implanted osmotic minipump (Alzet 2004, 0.25 μ l/h) filled with triple inhibitory cocktail (Muscimol/CNQX/dAP5, 0.6 mM/0.3 mM/2 mM, 3.6/1.8/12 nmol/day). A dummy cannula was implanted in the remaining external guide cannula, terminating 3 mm above the medial SuMN. The animals were returned to their home cage and received continuous infusion of triple cocktail at the medial SuMN for 10–14 days before electrophysiologic recording from the region. On the day of recording, the internal cannula connected to the minipump was removed and replaced with a fine tipped platinum iridium 150 micron recording electrode (FHC, #30046) with an impedance suited for multicellular recording (~0.8 M Ω). The dummy cannula was replaced with an internal cannula connected to microinjection pump (CMA/100), with 1 cc Hamilton syringe filled with 70 mM glutamate. The recording electrode was left in place for 30 min before recording. After baseline multiunit activity (quantified as average impulse per second for all cluster cut action potentials observed within the first two minutes of recording) was established, glutamate (70 mM) was delivered to the region via microinjector over a 1–2 min window at a rate of 0.5 μ l/min with or without subsequent triple cocktail infusion during which time multiunit action potential activity was recorded.

Data acquisition. After recording, action potentials were identified with a threshold discriminator, and then subsequently spike sorted using cluster analysis (LabChart 8, AD instruments, Colorado, catalog # MLU260M/8). Electrical signals were passed through an amplifier, surveyed through an AD instruments powerlab with NeuroEx signal conditioner (AD instruments, Colorado, catalog # FE185). Electrical signals were filtered at 0.3 Hz–5 kHz and sampled at 40 kHz. Spike detection was accomplished using a threshold discriminator and then cluster cutting of selected electrophysiologic signals was conducted offline with the use of Lab Chart 8 to isolate spike potentials from the background data (Nicollelis, 1999). Multi-unit activity was quantified as events per second for all selected spike potentials. Baseline multiunit activity at the medial SuMN area was quantified as the average firing rate (impulses per second) for all cluster cut action potentials observed within the one second testing window prior to iontophoretic injection of all test compounds and compared to the induced multiunit activity (impulses per second) observed between one and two seconds during iontophoretic injection of test compounds. Responses to test

compounds were measured as percent change in firing rate during the injection period relative to the pre-injection baseline.

Study 3: Comparative effect of GABA_A receptor agonist (Muscimol), glutamate AMPA/NMDA receptor antagonists (CNQX/dAP5) and their combination (Muscimol/CNQX/dAP5) infused at the medial SuMN area on glucose metabolism and body weight change

Rats fed regular chow were randomized to one of 4 groups (10 per group): Vehicle, Muscimol (GABA_A agonist), CNQX/dAP5 (AMPA/NMDA glutamate antagonists) or their combination (Muscimol/CNQX/dAP5). The rats received vehicle or one of these different drug infusions: Muscimol at 3.6 nmol/day or CNQX/dAP5 at 1.8/120 nmol/day at the medial SuMN via a chronically implanted osmotic mini pump (0.25 μ l/h) for 26 days. Following such treatments, fasting blood glucose and plasma insulin were measured after 6 h of fasting at ZT6–8 (*Zeitgeber* time; 6–8 hours after light onset) during the fasting period of the day. Body weight (BW) and food consumption were monitored during the study period. At the end of the experiment, rat brains were collected for histological verification of cannula placement.

Study 4: Effect of inhibition of neuronal activity at the medial SuMN area with local infusion of inhibitory cocktails on peripheral metabolism in HFD-resistant rats fed high fat diet

After a period of high fat feeding (one or four weeks in different studies), rats with % body weight gain less than the median % body weight gain were selected as high fat diet-resistant (HFD-r) and the other half with % body weight gain greater than the median % body weight gain were selected as high fat diet-sensitive (HFD-s) (Chang et al., 1990; Dourmashkin et al., 2006). Such selected HFD-r rats (specifically, % body weight gain < 7% after one week or < 22% after four weeks of HFD feeding, respectively) were maintained on HFD throughout the subsequent study period. *Study 4A*: HFD-r rats selected after one week of HFD feeding (BW = 289 \pm 5 g) were randomly assigned to one of 2 groups: vehicle (N = 10) or inhibitory dual cocktail (DC) (Muscimol/CNQX) (N = 12). Vehicle or DC (Muscimol/CNQX, 3.6/1.8 nmol/day) was locally infused at the medial SuMN area through an implanted osmotic mini pump (0.25 μ l/h) for three weeks. A glucose tolerance test (GTT) and a pyruvate tolerance test (PTT) (for details refer to GTT and PTT procedures and blood/plasma assays) were subsequently performed during the fasting period of the day (ZT6–8) to assess glucose tolerance, insulin sensitivity and hepatic glucose output. Food consumption and body weight were monitored during the study period. *Study 4B*: HFD-r rats selected after four weeks of HFD feeding (BW = 283 \pm 3.2 g) were randomly assigned to one of 2 groups: vehicle (N = 12) or inhibitory triple cocktail (TC) (Muscimol/CNQX/dAP5) (N = 12). Vehicle or TC (Muscimol/CNQX/dAP5, 3.6/1.8/120 nmol/day) was locally infused at the medial SuMN area through an

implanted osmotic mini pump (0.25 μ l/h) for two weeks. Then GTT was performed during the fasting period of the day (ZT6–8). Body weight and food consumption were monitored during the study period. At the end of the experiment, rats were sacrificed during the fasting period by decapitation. Parametrial and retroperitoneal white adipose tissue (pWAT and rWAT, respectively) were weighed and blood was collected for plasma triglyceride, insulin and leptin analyses.

Study 5: Effect of inhibition of neuronal activity at medial SuMN area with local infusion of inhibitory cocktails on peripheral metabolism in rats fed regular chow

Study 5A: HFD-sensitive (HFD-s) rats were selected based on % body weight gain greater than the medium % body weight gain (> 7%) after one week on HFD and were subsequently maintained on regular chow during the study period. Such selected HFD-s rats (BW = 306 \pm 4.4 g) were randomly divided into one of 2 groups: vehicle (N = 10) or DC (Muscimol/CNQX) (N = 12). Rats were locally infused at the medial SuMN area with vehicle or DC (Muscimol/CNQX, 3.6/1.8 nmol/day) through an implanted osmotic mini pump (0.25 μ l/h) for three weeks. A GTT was performed at the end of the experiment during the fasting period of the day (ZT6–8). Food consumption and body weight were monitored during the study period. *Study 5B*: Rats (BW = 247 \pm 4.1 g) without dietary pre-selection were fed regular chow and randomly assigned to one of 2 groups: vehicle (N = 22) or TC (Muscimol/CNQX/dAP5) (N = 22). Rats received local infusion at the medial SuMN area of vehicle or TC (Muscimol/CNQX/dAP5, 3.6/1.8/120 nmol/day) via an implanted osmotic mini pump (0.25 μ l/h) for four weeks. A GTT was performed at the end of the 4-week treatment during the fasting period of the day (ZT6–8). Body weight and food consumption were monitored throughout the study period. At the end of the experiment, half of each group of rats (Veh = 12; TC = 12) were sacrificed and parametrial and retroperitoneal white adipose tissue (pWAT and rWAT, respectively) were weighed. Liver was quickly frozen in liquid nitrogen for triglyceride content measurement. Blood was collected for plasma insulin and leptin analyses. The other half of each group of rats (Veh = 10; TC = 10) were sacrificed in pairs, and pWAT was freshly isolated for fatty acid-driven oxygen consumption rate (OCR) measurement.

Study 6: Delineation of the SuMN anatomical boundary of TC infusion effect upon metabolism

Rats (BW = 272 \pm 2.0 g) were fed regular chow and divided into one of 3 groups: medial SuMN site infusion with vehicle (N = 10); medial SuMN site infusion with TC (Muscimol/CNQX/dAP5, 3.6/1.8/12 nmol/day at 0.25 μ l/h) (N = 15); dorsal SuMN site infusion (1.5 mm dorsal to the medial SuMN) with TC (N = 10). End point data were collected after three weeks of treatment on body weight gain, food consumption, feed efficiency,

white adipose tissue (parametrial and retroperitoneal) weight and GTT glucose and insulin.

Study 7: Effect of circadian-timed daily activation of neuronal activity at the medial SuMN area with local infusion of NMDA or AMPA on HFD-induced metabolic syndrome

HFD-sensitive rats were selected based on % body weight gain greater than the medium % body weight gain (>22%) after four weeks of HFD feeding and were maintained on HFD for an additional two months. After a total of three months of HFD feeding, the rats were randomly assigned to one of 3 groups: Vehicle ($N = 10$), NMDA/D-serine ($N = 12$) or AMPA ($N = 12$). Vehicle, NMDA/D-serine (250/250 pmol/0.5 μ l) or AMPA (30 pmol/0.5 μ l) were daily infused at the medial SuMN area over 1 min through a chronically implanted guide cannula at ZT13 (near the time of onset of nocturnal locomotor activity, the circadian peak of overall SuMN activity, and the SuMN circadian peak of dopamine activity input at the SCN area) (Luo et al., 2018). After 2 weeks of treatment, a GTT was performed during the fasting period of the day (ZT6–8). Body weight and food consumption were monitored during the study period. At the end of the experiment, rats were sacrificed and parametrial and retroperitoneal white adipose tissues (pWAT and rWAT, respectively) were weighed and liver was quickly frozen in liquid nitrogen for liver triglyceride analysis. Blood was collected for plasma leptin and adiponectin analyses.

Histology

The cannula placement and the tissue distribution of acutely microinfused nigrosin (0.6 mM, 3 mM, or 10 mM in 0.5 μ l) and continuously infused fluorescent muscimol (0.6 mM, 0.25 μ l/h for 2–4 weeks) were examined and analyzed histologically. Nigrosin deposits were visualized under a dissection microscope (4 \times magnifications) and photographed on the brains sectioned coronally through the SuMN. For assessment of the tissue distribution of fluorescent muscimol after 2–4 weeks of continuous infusion, rats were anesthetized with ketamine/xylazine (80 mg/12 mg/kg, ip) and sacrificed by transcardiac perfusion with 4% paraformaldehyde. The brains were collected and post-fixed in 4% paraformaldehyde overnight and cryoprotected in 30% sucrose. The brains were then quickly frozen and sectioned on a cryostat at -20°C . Sequential coronal sections (35 μ m) were collected on a micro-slide and covered with VectorShield Medium with DAPI (Vector Lab, H1200). The fluorescent images were visualized and acquired using Lionheart FX automated microscope (BioTek Instrument, Inc) under Texas Red and DAPI filters. Exposure times were adjusted to maximize image quality and yet did not affect the visualized area of fluorescence. Measurement of the drug diffusion/tissue distribution was estimated from equally spaced 35 μ m sections.

Glucose tolerance test (GTT) and pyruvate tolerance test (PTT)

GTT was performed during the fasting period of the day (ZT6–8) by injecting rats with 50% dextrose solution (3 g/kg BW, ip; 2.5 g/kg BW, ip in Study 6). Blood samples were taken from the tail before and 30, 60, 90, 120 min after dextrose injection for blood glucose and plasma insulin analyses. PTT was similarly conducted via injecting 0.2 g/ml pyruvate solution (2 g/kg BW, ip), and tail blood was collected before and 30, 60, 90, 120 and 150 min after pyruvate injection for the analysis of glucose level.

Blood/plasma assay of metabolic parameters

Blood glucose was measured by a blood glucose monitor (OneTouch Ultra, LifeScan, Ins. Milpitas, California). Plasma insulin, leptin and adiponectin concentrations were determined by EIA using commercially available assay kits (ALPCO Diagnostics, Salem, NH): insulin ELISA (80-INSMR), leptin ELISA (22-LEPMS) and adiponectin ELISA (22-ADPRT). Belfiore insulin sensitivity index (ISI) (pmol/L*mmol/L*hr) was calculated based on the formula: $2/((\text{Insulin GTT AUC} * \text{Glucose GTT AUC}) + 1)$. HOMA insulin resistance (IR) was calculated based on the formula: $\text{fasting glucose (mmol/L)} \times \text{fasting Insulin (mU/L)}/22.5$. The plasma triglyceride (TG) was measured enzymatically by a TG Determination Kit (cat # TR0100, Sigma-Aldrich, St. Louis, MO). Hepatic triglyceride content was determined by extraction from liver tissue that was homogenized in 5% NP-40, heated to 90°C for 3 min, centrifuged at 10,000g for 10 min, and the supernatant subsequently assayed for triglyceride content by TG Determination Kit.

In vitro analysis of oxygen consumption rate (OCR) in adipocytes isolated from SuMNI-TC or vehicle treated rats

A 24-well format cell-based assay that measures fatty acid-driven oxygen consumption of adipocytes was conducted using the XFe24 Extracellular Flux Analyzer (Seahorse Bioscience, Agilent Technologies, Lexington, MA). Parametrial white adipose tissue (pWAT) was freshly dissected from a SuMN triple inhibitory cocktail treated rat and a vehicle treated (control) rat and placed in one XFe24 Islet Capture Microplate (8 mg/per well) in fatty acid oxidation assay medium. Oxygen Consumption Rate was assessed over 32 min at 37°C at baseline (basal) and in the subsequent presence of either 100 μ M Palmitate-Bovine Serum Albumin (BSA) or 400 μ M Etomoxir, a CPT-1 (carnitine palmitoyltransferase-1) inhibitor. Basal OCR was normalized as 100%. Exogenous fatty acid oxidation (Extra-FAO) was calculated as Palmitate-BSA OCR (%)-100 (baseline) and endogenous fatty acid oxidation (Endo-FAO) was calculated as 100 (baseline)-Etomoxir OCR (%) which represents non-fatty acid oxidation (Non-FAO). Relative basal OCR of the adipocytes from triple cocktail-treated rats vs the adipocytes from vehicle-treated rats was calculated. The data were

collected from 9 pairs of rats (triple cocktail vs vehicle) and analyzed using the software “Wave” (Agilent Technologies).

Data analysis

All data are expressed as mean \pm s.e.m. Two means were compared by two-tailed Student's t-test. More than two means were analyzed with one-way analysis of variance (ANOVA) followed by post-hoc two-tailed Student's t test to compare group difference. A p value less than 0.05 ($p < 0.05$) was accepted as statistically significant. Only rats with cannula tip localized inside, on the boundary of, or within 150 μ m dorsal from the medial SuMN were included in statistical analyses.

RESULTS

Study 1: Assessment of tissue distribution of GABA and glutamate receptor ligands at the medial SuMN area

Coronal brain section at the level of the SuMN as outlined by dotted lines is presented in low (Fig. 1A) and high (Fig. 1B) magnifications. Representative localizations of 13 infusion cannula tips (inside and within 150 μ m from the dorsal boundary of the medial SuMN) that were included in statistical analyses are illustrated on a brain coronal sketch (Fig. 1C). The tip location of the infusion cannula employed in the present studies was visualized at the medial SuMN (Fig. 1D–J). Firstly, the tissue distribution of acutely infused 0.5 μ l of black nigrosin at 0.6 mM, 3 mM or 10 mM examined at 3 h post-infusion was primarily confined within the medial SuMN even at a dose of 20-fold the highest employed dose of receptor ligands (Fig. 1D–F). The lateral SuMN and mammillary bodies were clear and the supramammillary decussation area dorsal to the SuMN was substantially clear of black stain. No nigrosin stain was detected in the adjacent anterior VTA. Very limited diffusion along the cannula tract dorsal to the SuMN was detected with a nigrosin dose of 3 mM (6-fold higher than the dose of receptor ligands used in this study). Secondly, the red fluorescent signal of fluorescent muscimol (0.6 mM) after continuous microinfusion for 2 and 4 weeks was found confined within the medial SuMN area restricted to \sim 0.5 mm from the infusion site (tip of infusion cannula) (Fig. 1G–J). Such red fluorescent signal was not detected above background in the adjacent posterior hypothalamic area including the lateral SuMN or the mammillary body ventrally. The supramammillary decussation area was also substantially free of such signal (Fig. 1G–J). The adjacent anterior VTA was clear of red fluorescent signal. A similar localized pattern of brain nigrosin staining was observed following the same chronic infusion at the same dose as fluorescent muscimol (data not shown).

Study 2: Effect of glutamate and GABA_A receptor ligands and their combinations on multi-unit firing rates in the medial SuMN area

Compared with baseline multiunit activity, iontophoretic application of glutamate elicited a significant increase (299%, $p < 0.05$) in multiunit activity observed in the medial SuMN area (Fig. 2A), as did iontophoretic application of AMPA (241%, $p < 0.05$) (Fig. 2B) and of NMDA/D-serine (574%, $p < 0.05$) (Fig. 2C). By contrast, multiunit activity within the medial SuMN area was significantly reduced by the application of Muscimol (94%, $p < 0.05$) (Fig. 2D), CNQX (83%, $p < 0.05$) (Fig. 2E), and dAP5 (74%, $p < 0.05$) (Fig. 2F). Similar inhibitory effects were observed from the iontophoretic injection of a combination of Muscimol and CNQX (inhibitory dual cocktail [DC]) resulting in a significantly reduced (75%, $p < 0.05$) multiunit activity rate (Fig. 2G), and moreover, following the injection of a combination of Muscimol, CNQX and dAP5 (inhibitory triple cocktail [TC]) which also resulted in a significantly reduced (94%, $p < 0.05$) multiunit activity rate (Fig. 2H). The inhibitory effects observed from delivery of TC, though numerically larger than those of DC, did not differ significantly from those seen following delivery of DC ($p = 0.21$).

In rats that received continuous intra-SuMN infusion of TC for 10–14 days, there was a significant increase in the multi-unit activity rate during the application of glutamate (baseline mean MUA = 1.2 spikes/second, glutamate induced mean MUA = 8.5 spikes/second, paired t-test $p < 0.01$) (Fig. 2I, J). The glutamate induced firing was challenged in some cases by subsequent delivery of TC to the same region. When tested, this inhibitory challenge resulted in a dramatic reduction of increase in the multi-unit activity rate (glutamate induced mean MUA = 4.7 spikes/second, TC challenged MUA = 0.15 spikes/second). These findings indicate that while the chronic TC infusion inhibits SuMN neuronal activity, these neurons are not damaged by such infusion in any manner that makes them either unresponsive to glutamate stimulation or subsequent acute inhibition in response to TC administration.

Study 3: Comparative metabolic effect of GABA_A receptor agonist, glutamate AMPA/NMDA receptor antagonists and their combination at the medial SuMN area

The effect of local infusion at the medial SuMN of GABA_A receptor agonist (Muscimol), glutamate AMPA/NMDA receptor antagonists (CNQX/dAP5) or their combination (triple cocktail) (Muscimol/CNQX/dAP5) on glucose metabolism and body weight change was compared in rats maintained on regular diet. After 26 days of treatment, compared with vehicle, % body weight gain was increased by Muscimol (13.6% vs 7.2% in vehicle, $p = 0.008$) and by the triple cocktail (14% vs 7.2% in

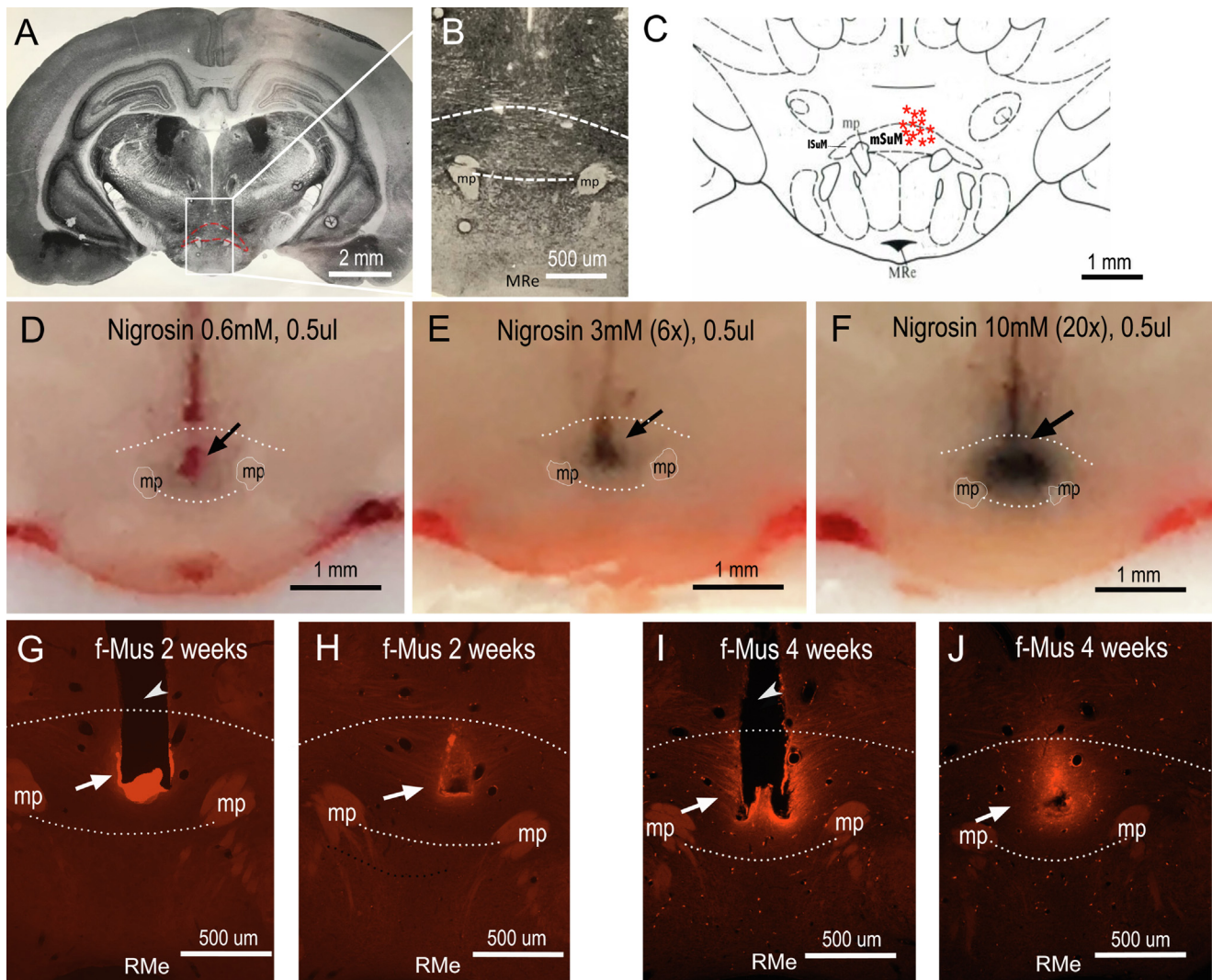


Fig. 1. Cannula placement and drug diffusion following acute and chronic infusion demonstrate drug confinement to the medial SuMN area. **(A)** Coronal section at the level of SuMN (Bregma – 4.52 mm). The contour of the SuMN perimeter is indicated by dotted lines. **(B)** High magnification of the medial SuMN region. **(C)** The coronal brain sketch showing 13 representative cannula placements (red asterisks) at the medial SuMN area. **(D–F)** Nigrosin staining after acute microinfusion of 0.5 μ l nigrosin at molar concentrations comparable to (0.6 mM) **(D)** or greater (3 mM [6X]; 10 mM [20X]) **(E–F)** than the highest concentration of acutely infused glutamate receptor ligands (i.e., NMDA, 0.5 mM, 0.5 μ l) used in the experiments. The medial SuMN area is indicated by dotted lines. Black deposits from 0.6 mM nigrosin were detected within the medial SuMN area with little spread to the lateral SuMN or surrounding regions **(D)**. **(G–J)** Red fluorescence of fluorescent muscimol (f-Mus) (0.6 mM) following its microinfusion through an osmotic pump (0.25 μ l/h) at the medial SuMN area for two weeks **(G, H)** and four weeks **(I, J)**. On sections cut through the core **(G, I)** and the outside border of the cannula **(H, J)**, red fluorescence was detected at the medial SuMN area primarily restricted to \sim 0.5 mm from the tip of cannula. Little spread of f-Mus to the lateral SuMN or surrounding region was detected. mp, mammillary peduncle; MRe, mammillary recess; 3V, 3rd ventricle; mSuM, medial supramammillary nucleus; ISuM, lateral supramammillary nucleus; arrows indicate tip of cannula; arrow heads indicate cannula track. (For interpretation of the references to colour in this figure legend, the reader is referred to the web version of this article.)

vehicle, $p = 0.005$) but not by CNQX/dAP5 (Fig. 3B). The average daily food consumption/per rat over the study period was increased only in the triple cocktail treated rats (15%, $p = 0.012$) (Fig. 3C). As a result, the feed efficiency (g BW gain per gram of food consumed over the study period/per rat) was increased in triple cocktail (69%, $p = 0.007$) and Muscimol (75%, $p = 0.01$) treated rats but not in CNQX/dAP5 treated rats (Fig. 3D). All three SuMNi treatments elevated HOMA-IR index indicating development of insulin resistance (Muscimol, 69%, $p = 0.008$; CNQX/dAP5, 44%, $p = 0.025$; triple cocktail, 53%, $p = 0.003$) relative to

vehicle (Fig. 3G). However, only the triple cocktail treatment significantly increased both fasting blood glucose (9%, $p = 0.017$) and plasma insulin (44%, $p = 0.009$), while Muscimol alone increased plasma insulin (64%, $p = 0.007$) without effect on blood glucose and CNQX/dAP5 increased blood glucose (14%, $p = 0.001$) without effect on plasma insulin (Fig. 3E, F). Based on these results, all subsequent SuMN inhibition studies employed a cocktail of GABA_A receptor agonist plus AMPA receptor antagonist (Muscimol/CNQX, termed SuMN inhibitory dual cocktail [SuMNi-DC] or [DC]) or GABA_A receptor agonist plus

AMPA and NMDA receptor antagonists (Muscimol/CNQX/dAP5, termed SuMN inhibitory triple cocktail [SuMNI-TC] or [TC]) to study such inhibitory effect of SuMN neuronal activity on peripheral fuel metabolism.

Study 4: Inhibition of neuronal activity at the medial SuMN area induces obesity, insulin resistance and glucose intolerance in HFD-resistant rats fed HFD

Study 4A: Inhibition of medial SuMN neuronal activity of HFD-resistant rats fed HFD by continuous local infusion of SuMNI-DC (Muscimol/CNQX) for three weeks induced insulin resistance and impaired glucose tolerance without change in body weight or fat mass. Compared with the vehicle treated group, Muscimol/

CNQX increased GTT glucose area under curve (AUC) by 22% ($p = 0.043$) (Fig. 4A, B) and insulin AUC by 154% ($p = 0.002$) (Fig. 4C, D). As a result, Belfiore insulin sensitivity index (ISI) was decreased by 59% ($p = 0.0001$) indicating that Muscimol/CNQX treatment induced insulin resistance (Fig. 4E). During a pyruvate tolerance test, Muscimol/CNQX treatment induced a significant elevation in plasma glucose levels at 90 (29%, $p = 0.035$), 120 (38%, $p = 0.01$) and 150 (35%, $p = 0.014$) minutes after pyruvate injection (Fig. 4F). Thus, infusion of Muscimol/CNQX at the medial SuMN induced glucose intolerance, insulin resistance and an increase in hepatic glucose output. The increases in body weight and food consumption induced by Muscimol/CNQX did not reach significance ($p = 0.9$ and 0.13 , respectively) compared with vehicle (Fig. 4G, H).

Study 4B: Inhibition of medial SuMN neuronal activity of HFD-resistant rats fed HFD by chronic local infusion of SuMNI-TC (Muscimol/CNQX/dAP5) for two weeks induced insulin resistance, impaired glucose tolerance, and obesity. Compared with the vehicle treated group, the SuMNI-TC treatment increased glucose AUC by 43% ($p = 0.007$) (Fig. 5A, B) without change in insulin AUC during GTT (Fig. 5C, D). Belfiore ISI was significantly decreased by 44% ($p = 0.038$) indicating insulin resistance (Fig. 5E). Moreover, body weight gain in the SuMNI-TC group was 3.7 fold greater than the vehicle group (11% increase vs 3% increase in vehicle group, $p = 0.001$) (Fig. 5F, G), which was accompanied by an increase in white adipose tissue (WAT) weight (parametrial pWAT by 73%, $p = 0.004$; retroperitoneal

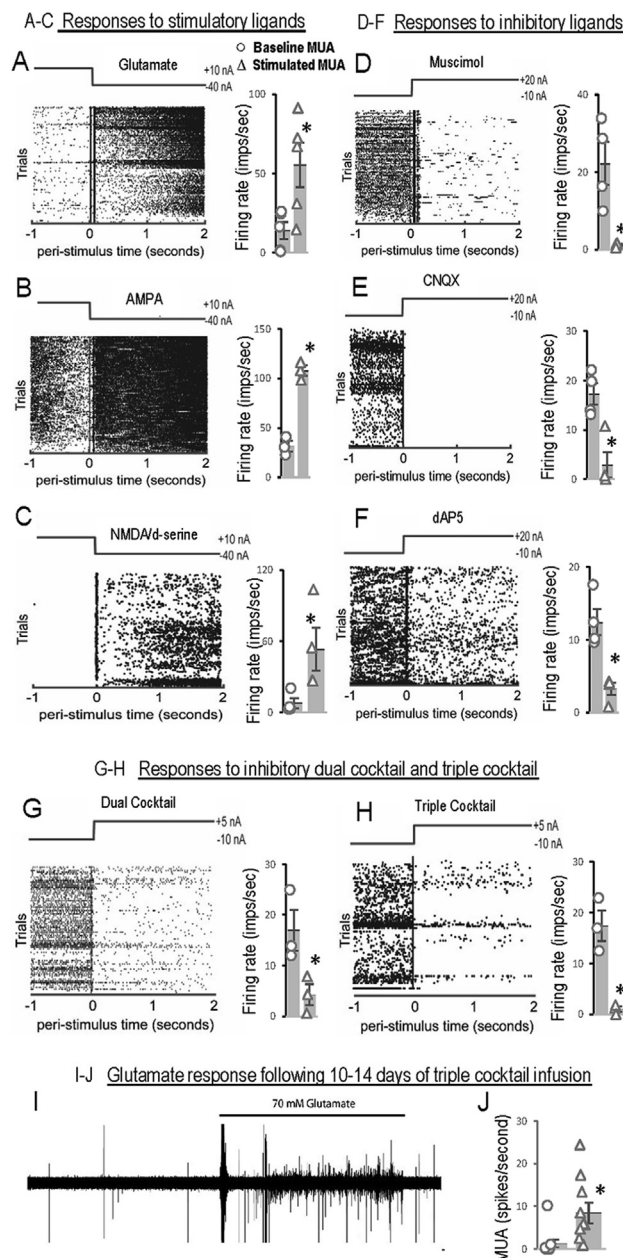


Fig. 2. Electrophysiological response of medial SuMN area to applications of glutamate and/or GABA_A receptor ligands on multi-unit neuronal activity verify their neuronal stimulatory and inhibitory effect, respectively therein. (A–H) Depict the acute electrophysiological effects of iontophoretically applied receptor ligands in naive animals. ((A) Left) Example peri-event rasters of multi-unit activity (MUA) in the medial SuMN area from a single representative animal for 1 s prior and 2 s during iontophoretic injection of glutamate. Each dot shows a cluster cut action potential from any one of the many neurons proximal to the tip of the recording electrode. Trials, the y-axis, depict each successive repetition of baseline, and stimulation recording from a single animal following a brief rest period in between trials. ((A) Right) Population average from all animals in the group receiving iontophoretic application of glutamate ($n = 5$), baseline activity rate in the medial SuMN area obtained 1 s prior to injection (circles) and induced activity (triangles) measured from 1 to 2 s after the start of iontophoretic injection of glutamate. Remaining panels B–H follow the same format. Response of SuMN MUA to iontophoretically applied AMPA ((B) $n = 3$), NMDA/d-serine ((C) $n = 4$), Muscimol (GABA_A receptor agonist) ((D) $n = 3$), CNQX (AMPA receptor antagonist) ((E) $n = 4$), and dAP5 (NMDA receptor antagonist) ((F) $n = 3$). (G) Response of SuMN MUA to simultaneous iontophoretically injected CNQX and Muscimol (dual cocktail, $n = 3$), and (H) the response to simultaneous iontophoretically injected CNQX, Muscimol and dAP5 (triple cocktail, $n = 3$). (I, J) Show the acute effects of glutamate pressure injected in the medial SuMN area of animals who have received 10–14 days of triple cocktail treatment. (I) Representative example recording showing 2 min of baseline activity, followed by 2 min of glutamate induced activity. (J) Population average ($n = 11$) of multi-unit firing rates during baseline (circles) and glutamate induced activity (triangles). *Significance, $p < 0.05$.

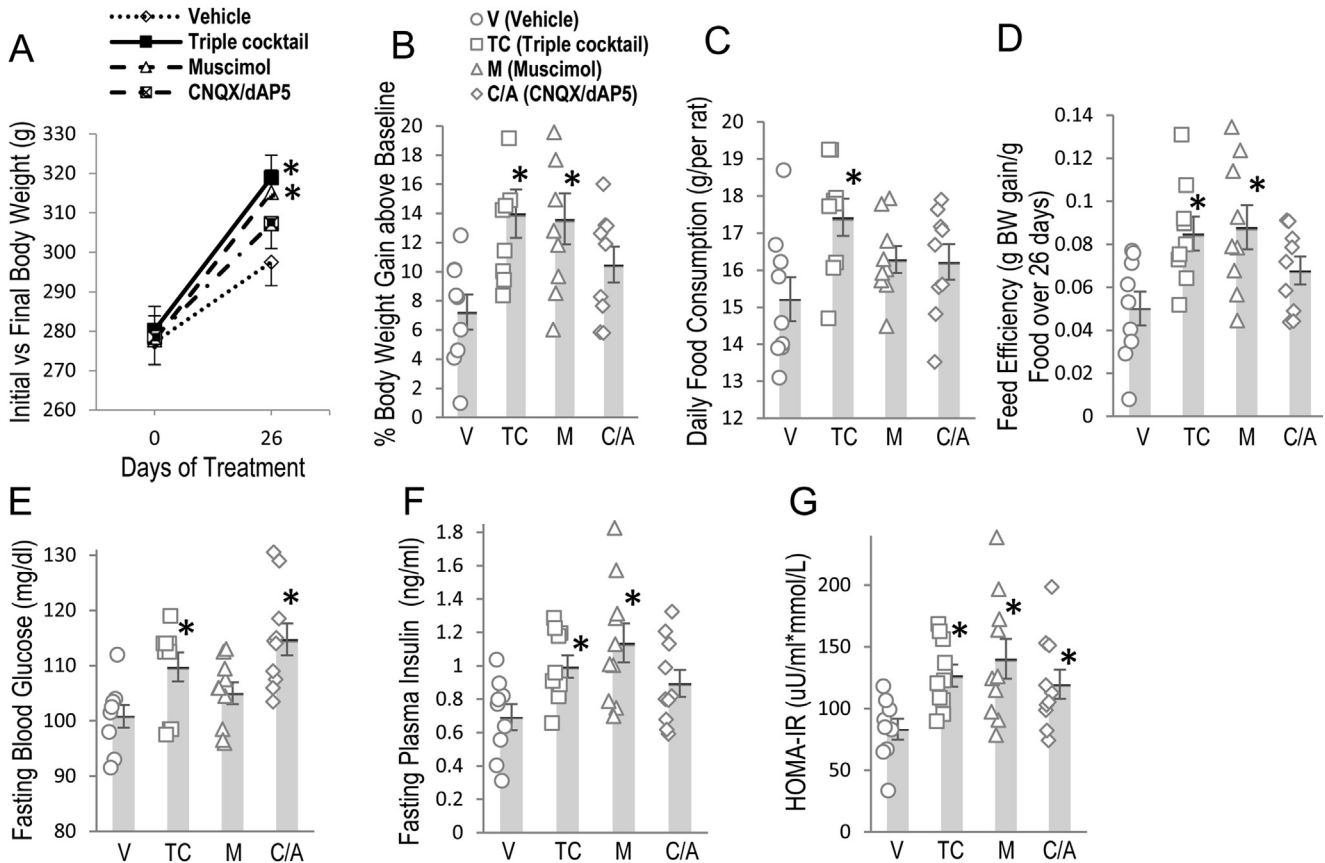


Fig. 3. Comparative effects of SuMN inhibition with GABA_A agonist (Muscimol), AMPA/NMDA antagonists (CNQX/dAP5) and combination (Muscimol/CNQX/dAP5) on metabolism. Rats fed regular chow were infused locally at medial SuMN area with vehicle, Muscimol (3.6 nmol/day), CNQX/dAP5 (1.8/120 nmol/day) or their combination (triple cocktail [TC]) (Muscimol/CNQX/dAP5) (3.6/1.8/120 nmol/day) for 26 days. Compared with vehicle, % body weight gain was increased by Muscimol (13.6% vs 7.2% in vehicle, $p = 0.008$) and TC (14% vs 7.2% in vehicle, $p = 0.005$) but not by CNQX/dAP5 (**A, B**). Daily food consumption was increased by TC ($p = 0.012$) only (**C**). Feed efficiency (g body weight gain/g food consumed during the study period/per rat) was increased by Muscimol ($p = 0.01$) and TC ($p = 0.007$) but not by CNQX/dAP5 (**D**). Both fasting glucose ($p = 0.017$) and fasting insulin ($p = 0.009$) were increased by TC, while Muscimol increased fasting insulin ($p = 0.007$) and CNQX/dAP5 increased fasting glucose ($p = 0.001$) only (**E, F**). The HOMA-IR index was increased by Muscimol ($p = 0.008$), CNQX/dAP5 ($p = 0.025$) and TC ($p = 0.003$) (**G**). *Significance, $p < 0.05$.

rWAT by 69%, $p = 0.005$; total tl WAT by 72%, $p = 0.004$) (**Fig. 5H**), and in cumulative HFD food consumption (32%, $p = 0.0002$) (**Fig. 5I, J**). Coincidentally, feeding efficiency was increased by the SuMNI-TC (111%, $p = 0.009$) compared with vehicle (**Fig. 5K**). SuMNI-TC induced hyperinsulinemia (162%, $p = 0.03$) without change in fasting glucose, and induced fasting insulin resistance as reflected by an increase in HOMA-IR (169%, $p = 0.043$) (**Fig. 5L–N**). Plasma leptin and plasma triglyceride levels were also increased by 163% ($p = 0.002$) and 75% ($p = 0.02$) respectively (**Fig. 5O, P**) by SuMNI-TC treatment.

Study 5: Inhibition of neuronal activity at the medial SuMN area induces obesity and insulin resistance in rats fed regular chow

Study 5A: Inhibition of medial SuMN neuronal activity of HFD-sensitive rats fed regular chow by continuous local infusion of a SuMNI-DC (Muscimol/CNQX) for three weeks induced insulin resistance without change in body weight. Compared to vehicle control, SuMNI-DC

increased the GTT plasma insulin AUC by 125% ($p = 0.032$) (**Fig. 6C, D**) without significantly increasing glucose AUC (11%, $p = 0.14$) (**Fig. 6A, B**). Belfiore ISI was decreased by 39% ($p = 0.01$) (**Fig. 6E**) indicating that such SuMNI-DC treatment induced insulin resistance. The change in body weight and food consumption induced by Muscimol/CNQX did not reach significance compared with vehicle (**Fig. 6F, G**).

Study 5B: Inhibition of medial SuMN neuronal activity of regular chow-fed rats without dietary pre-selection by continuously local infusion of SuMNI-TC (Muscimol/CNQX/dAP5) for four weeks induced insulin resistance and obesity. Compared with vehicle treated rats, SuMNI-TC treatment significantly increased GTT insulin area under the curve (AUC) (163%, $p = 0.009$) (**Fig. 7C, D**) with no change in glucose AUC (**Fig. 7A, B**). Belfiore ISI was significantly decreased by 42% ($p = 0.028$) indicating insulin resistance (**Fig. 7E**). Furthermore, SuMN inhibition with the TC increased body weight gain by 2.3 fold (21% increase verses 9% increase in the vehicle group, $p < 0.0001$) (**Fig. 7F, G**) and increased pWAT by 117% ($p < 0.0001$), rWAT by

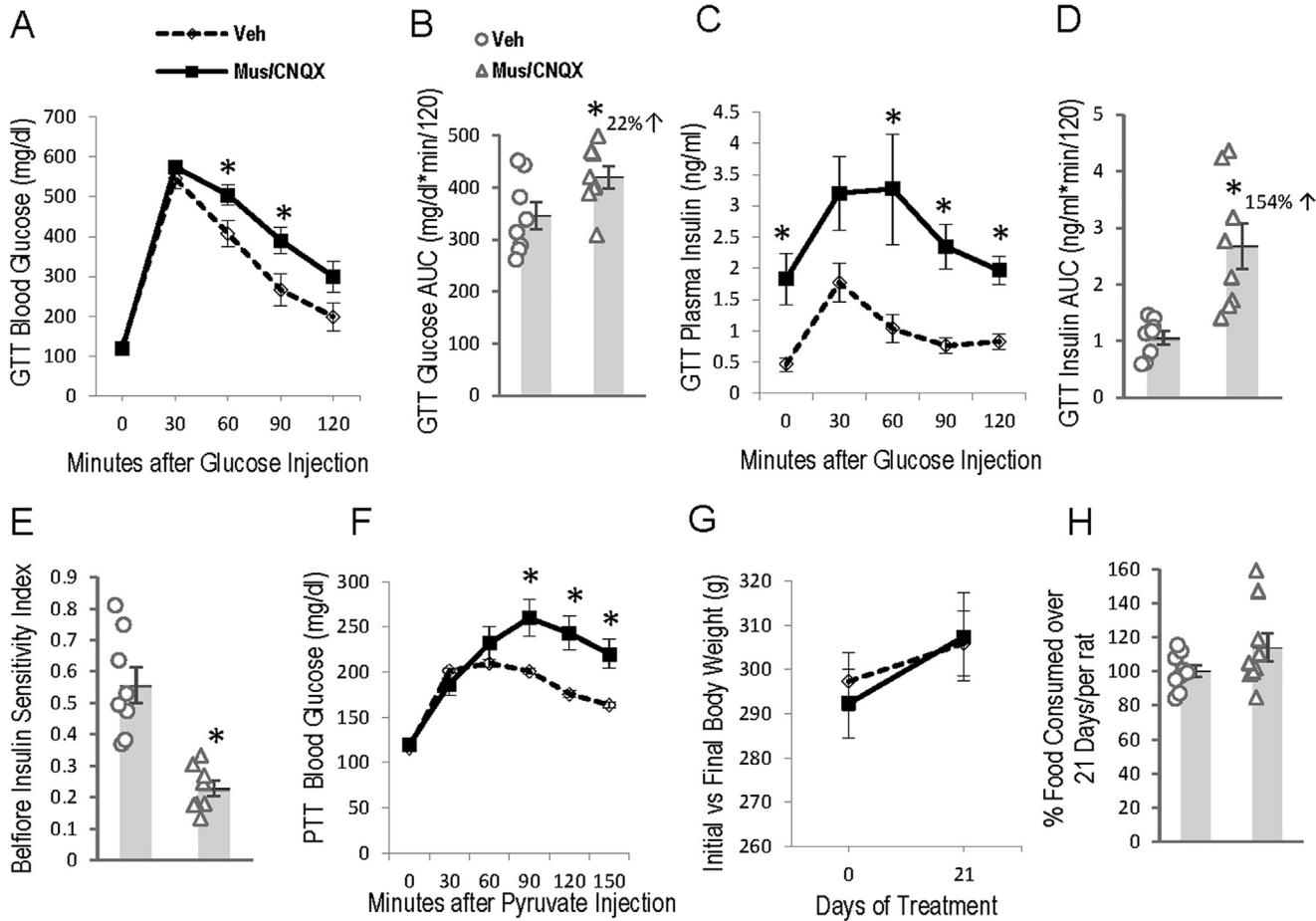
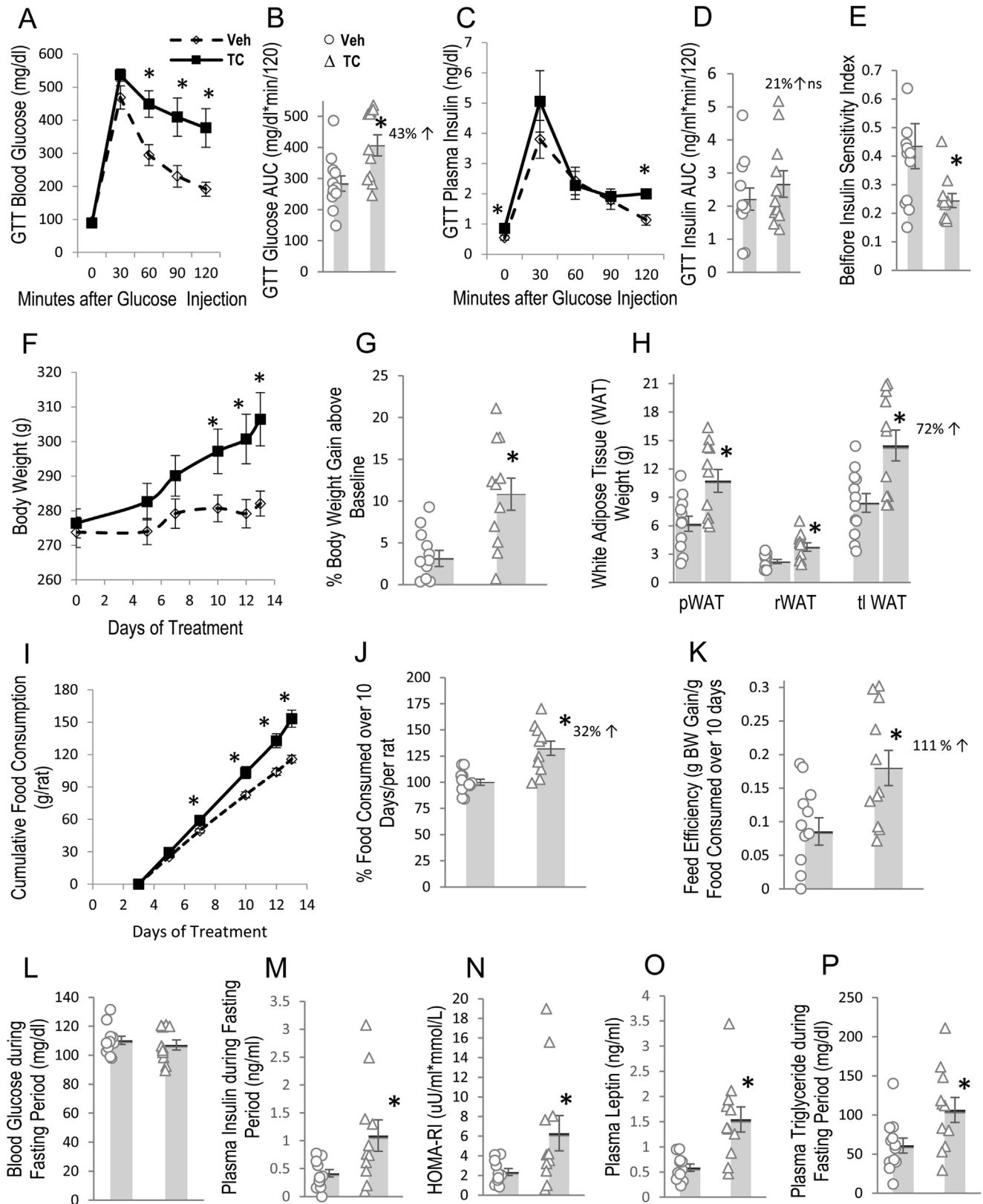


Fig. 4. SuMN inhibition with Dual Cocktail induces insulin resistance/glucose intolerance in HFD-resistant rats fed HFD. HFD-resistant rats fed HFD were locally infused at medial SuMN area with vehicle or dual cocktail (Muscimol[Mus]/CNQX, 3.6/1.8 nmol/day) for 3 weeks. Compared with vehicle, Mus/CNQX increased GTT glucose AUC (22%, $p = 0.043$) (A, B) and insulin AUC (154%, $p = 0.002$) (C, D) resulting in a significant reduction in Belfiore insulin sensitivity index (59%, $p = 0.0001$) (E). A pyruvate tolerance test (PTT) revealed a Mus/CNQX-induced elevation of plasma glucose by 29% ($p = 0.035$), 38% ($p = 0.01$) and 35% ($p = 0.014$) at 90, 120 and 150 min after pyruvate injection respectively (F). The increase in body weight (G) and food consumption (H) induced by Mus/CNQX did not reach significance compared to vehicle. *Significance, $p < 0.05$.

85% ($p = 0.0004$) and tl WAT by 107% ($p < 0.0001$) (Fig. 7H). Such SuMNI-TC induced increases in body weight and body fat were accompanied by an increase in total cumulative food consumption (21%, $p < 0.0001$) (Fig. 7I, J) and an increase in feed efficiency (85%, $p < 0.0001$) (Fig. 7K). SuMN inhibition with TC induced a slight but significant increase in blood glucose (8%, $p = 0.008$) (Fig. 7L), marked hyperinsulinemia (123% increase, $p = 0.0004$) (Fig. 7M) and fasting insulin resistance as assessed by an increased HOMA-IR (145%, $p = 0.0004$) (Fig. 7N). Such SuMNI-TC treatment also increased plasma leptin level (126%, $p = 0.004$) (Fig. 7O) and liver triglyceride content (55%, $p = 0.002$) (Fig. 7P). Compared with vehicle, the basal oxygen consumption rate in pWAT was significantly reduced by 42% ($p = 0.004$) in the triple cocktail treated animals (Fig. 7Q) with no reduction in endogenous or exogenous fatty acid oxidation (data not shown).

Study 6: Verification of site-specific effect of inhibitory triple cocktail at the medial SuMN area

To further delineate the possible contribution of off-target (non-SuMN) chronic TC infusion on study results, we compared the metabolic impact of such TC infusion at an area 1.5 mm dorsal to the medial SuMN with those of TC infusion at the medial SuMN area in rats maintained on regular chow diet. Compared with vehicle, TC (Muscimol/CNQX/dAP5, 3.6/1.8/12 nmol/day) infusion for 3 weeks at the medial SuMN area (TC-SuMN), but not at an area 1.5 mm dorsal to the medial SuMN (TC-dorsal), increased GTT insulin AUC (42%, $p = 0.021$) (Fig. 8C, D) with 0.4% reduction in Belfiore insulin sensitivity index ($p = 0.05$) (Fig. 8E); increased% body weight gain by 2.1 fold (12% vs 5.7% increase in vehicle group, $p = 0.006$) (Fig. 8F, G) and WAT weight (pWAT by 57%, $p = 0.017$; rWAT by 52%, $p = 0.03$; and tl WAT by 56%, $p = 0.018$)



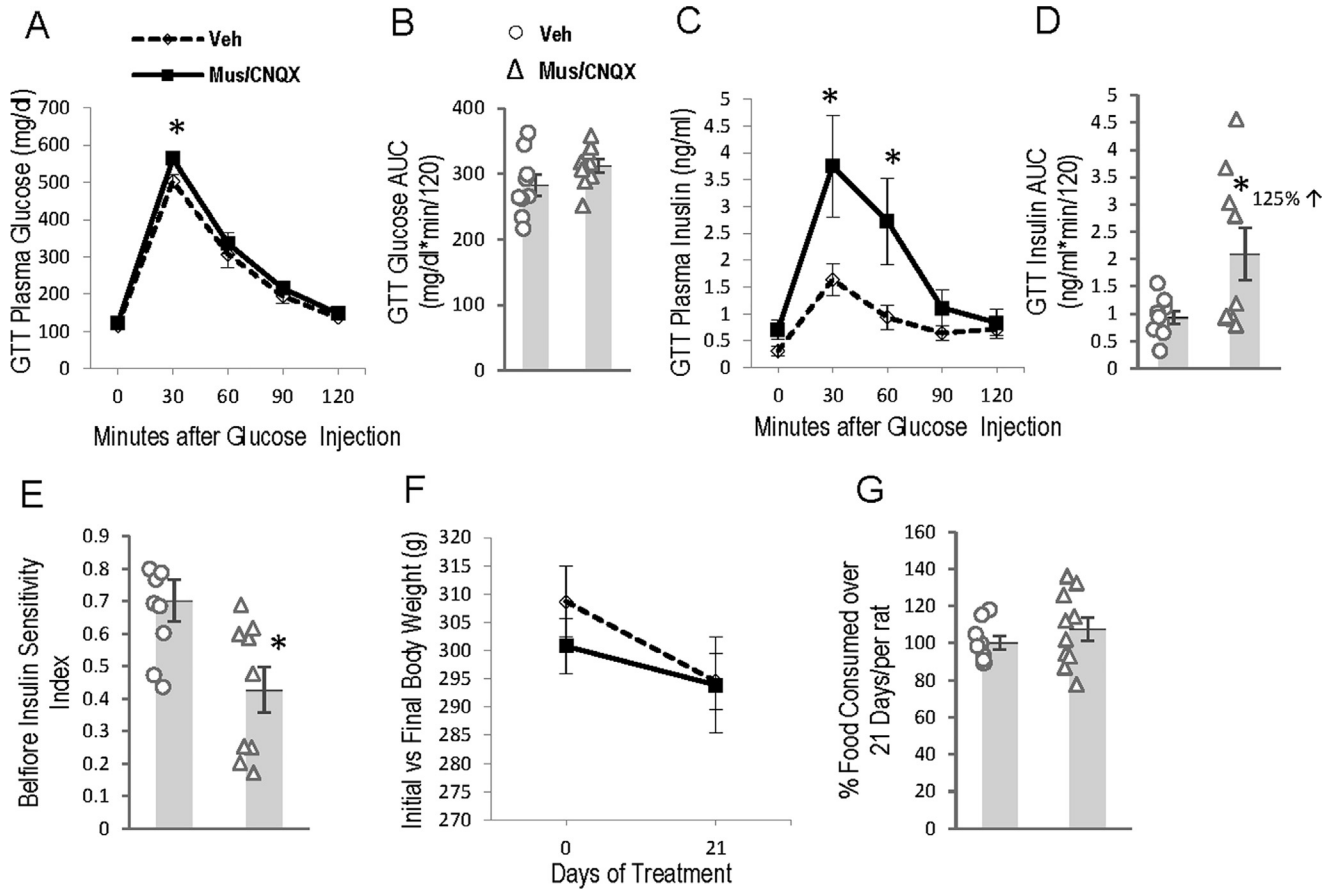


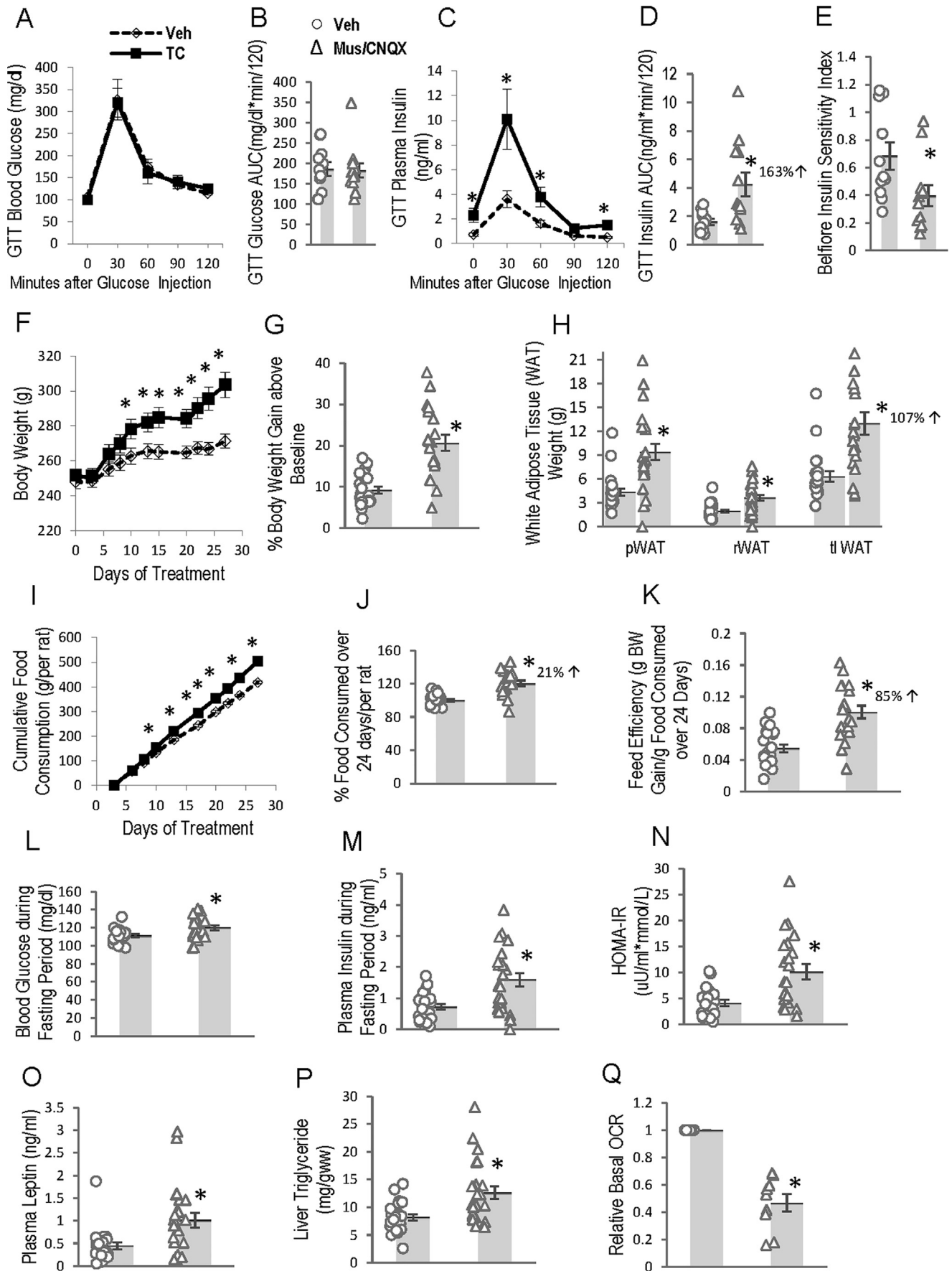
Fig. 6. SuMN inhibition with Dual Cocktail induces insulin resistance in HFD-sensitive rats fed regular chow. HFD-sensitive rats fed regular chow received continuous local infusion at medial SuMN area with vehicle or dual cocktail (Muscimol [Mus]/CNQX, 3.6/1.8 nmol/day) for three weeks. Compared to vehicle, Mus/CNQX increased GTT insulin AUC by 125% ($p = 0.032$) (C, D) with no significant increase in glucose AUC (11%, $p = 0.14$) (A, B) resulting in 39% reduction in Belfiore insulin sensitivity index ($p = 0.01$) (E). There was no change in body weight (F) or food consumption (G). *Significance, $p < 0.05$.

(Fig. 8H); increased food consumption (14 %, $p = 0.004$) (Fig. 8I, J) and increased feed efficiency (85%, $p = 0.004$) (Fig. 8K). Furthermore, compared with TC-dorsal infused rats, TC-medial SuMN infused rats had increased % body weight gain by 2.2 fold (12% vs 5.5% increase in TC-dorsal group, $p = 0.004$) (Fig. 8F, 8G), WAT weight (pWAT by 73%, $p = 0.016$; rWAT by 69%, $p = 0.018$; tl WAT by 72%, $p = 0.015$) (Fig. 8H), food consumption (12%, $p = 0.006$) (Fig. 8I, J) and feed efficiency (96%, $p = 0.003$) (Fig. 8K). Thus, infusion of the TC at 1.5 mm dorsal to the medial SuMN produced no significant changes in any metabolic parameters tested versus control animals.

Study 7: Circadian-timed daily activation of neuronal activity at the medial SuMN area improves HFD-induced metabolic syndrome

We further examined whether circadian-timed activation of medial SuMN area could improve insulin resistance and metabolic abnormalities in HFD-sensitive, HFD-induced insulin resistant animals. The neuronal activity at the medial SuMN area was stimulated with daily local infusion of AMPA or NMDA (0.5 μ l over 1 min) at the beginning of nocturnal onset of locomotor activity (the circadian peak of SuMN neuronal activity in healthy animals) (ZT13) for two weeks. Compared with vehicle

Fig. 5. SuMN inhibition with Triple Cocktail (TC) induces obesity, insulin resistance/glucose intolerance in HFD-resistant rats fed HFD. HFD-resistant rats fed HFD were locally infused at medial SuMN area with vehicle or TC (Muscimol/CNQX/dAP5, 3.6/1.8/120 nmol/day) for two weeks. Compared with vehicle, TC increased GTT glucose AUC (43%, $p = 0.007$) (A, B) with no change in insulin AUC (C, D) resulting in 44% reduction in Belfiore insulin sensitivity index ($p = 0.038$) (E). TC increased body weight gain by 3.7 fold (11% increase vs 3% increase in vehicle group) ($p = 0.001$) (F, G). TC-treated rats consumed 32% more HFD than the vehicle group ($p = 0.0002$) (I, J) and exhibited 111% increase in feed efficiency (g body weight gain/g food consumed during the study period/per rat, $p = 0.009$) (K) coupled with an increase in white adipose tissue (WAT) weight (parametrial pWAT by 73%, $p = 0.004$; retroperitoneal rWAT by 69%, $p = 0.005$ and total tl WAT by 72%, $p = 0.004$) (H). TC induced fasting hyperinsulinemia (162%, $p = 0.03$) with little change in blood glucose resulting in an increased HOMA-IR (169%, $p = 0.043$) (L–N), and increased plasma leptin by 163% ($p = 0.002$) (O) and plasma triglyceride by 75% ($p = 0.02$) (P). *Significance, $p < 0.05$. ns: not significant.



treated rats, AMPA did not alter GTT glucose AUC (Fig. 9A, E), but reduced GTT insulin AUC by 33% ($p = 0.031$) (Fig. 9B, F). As a result, Belfiore ISI was significantly increased by 58% ($p = 0.016$) (Fig. 9G) indicating an improvement in insulin sensitivity. NMDA treatment as compared with vehicle decreased GTT glucose AUC by 26% ($p = 0.016$) (Fig. 9C, E) with no significant reduction in insulin AUC (23%, ns, $p = 0.065$) (Fig. 9D, F) resulting in a significant increase in Belfiore ISI (58%, $p = 0.009$) indicating an improvement in insulin sensitivity (Fig. 9G). The improvement in insulin sensitivity by such AMPA or NMDA treatment was not accompanied by significant reduction in body weight (Fig. 9I) or food consumption (Fig. 9J). Nevertheless, NMDA but not AMPA significantly reduced WAT weight (pWAT by 28%, $p = 0.01$; rWAT by 33%, $p = 0.041$; tl WAT by 30%, $p = 0.015$) (Fig. 9H). Furthermore, NMDA treatment but not AMPA also significantly reduced plasma leptin (62%, $p = 0.0001$) (Fig. 9K) and liver triglyceride (31%, $p = 0.016$) (Fig. 9L) while plasma adiponectin was significantly increased by both NMDA (247%, $p = 0.0001$) and AMPA (355%, $p < 0.0001$) treatment (Fig. 9M). Compared with AMPA, NMDA treatment reduced plasma leptin (49%, $p = 0.001$) (Fig. 9K) and liver triglyceride (28%, $p = 0.002$) (Fig. 9L).

DISCUSSION

This study is the first to demonstrate that chronic inhibition of medial SuMN area neuronal activity (via GABAa receptor agonist plus glutamate receptor antagonist treatment) or circadian-timed activation of medial SuMN area neuronal activity (via NMDA or AMPA agonist treatment) is capable of inducing or reversing, respectively, the insulin resistance syndrome in animals. Such neurophysiological manipulations produced marked alterations in peripheral fuel metabolism including insulin sensitivity, glucose tolerance, liver lipid biochemistry, adipocyte oxygen consumption rate, body composition, food consumption and feed efficiency thus identifying the medial SuMN area as a novel metabolic regulatory locus in the posterior hypothalamus. Chronic inhibition of neuronal activity at the medial SuMN area (SuMNI) via local application of GABAa receptor agonist plus NMDA and AMPA glutamate receptor antagonists, each known to inhibit neuronal activity (Broadbent et al., 2010; Gliddon et al., 2005; Maalouf et al., 1998) and demonstrated herein to do so at the SuMN, potentiated

the detrimental metabolic effects of high fat diet including hyperinsulinemia, insulin resistance, glucose intolerance, obesity, increased food consumption, increased feed efficiency, hyperleptinemia, and elevated plasma and liver triglyceride levels in animals otherwise refractory to such an effect of HFD. Moreover, such SuMNI treatment produced similar metabolic results in animals maintained on a low fat diet including induction of hyperinsulinemia, insulin resistance, increased feeding and feed efficiency, obesity, increased fat liver storage, hyperleptinemia and hyperlipidemia. However, such SuMNI-induced glucose intolerance required the presence of a HFD (see Fig. 4A [HFD] vs 6A [regular chow]; Fig. 5A [HFD] vs 7A [regular chow]). Consistent with such SuMNI findings is the observation that circadian-timed activation of neuronal activity at the medial SuMN area with either the glutamate NMDA or AMPA receptor agonist in HFD sensitive, obese, insulin resistant animals attenuated this condition, though with NMDA receptor agonist being noticeably more potent than AMPA receptor agonist in this regard.

The receptor ligand tissue distribution tracking studies conducted herein strongly suggest that the concentrations of acutely and chronically administered doses of GABAa agonists and NMDA and AMPA agonists and antagonists were nearly exclusively confined to the medial SuMN area. We also observed a similar metabolic impact of fluorescent muscimol when infused at medial SuMN area to that of unlabeled muscimol. Moreover, when the infusion cannula was positioned 1.5 mm dorsal from the medial SuMN and even closer to the floor of the 3rd ventricle, no metabolic impact was detected by the inhibitory triple cocktail infusion (Study 6). Nevertheless, the receptor ligands infused at the medial SuMN area could potentially act on input neuronal terminals and fibers of passage in addition to SuMN neurons. Therefore, discussion of results herein is of the treatment impact upon the medial SuMN area and not of the medial SuMN exclusively.

Several neuropharmacological specifics of the current study results are worthy of further discussion as follows. Firstly, each of either GABAa agonist or glutamate AMPA plus NMDA antagonists at the medial SuMN area contributed to the genesis of the obese, insulin resistant state in animals held on a low fat diet with the combination of such GABA and glutamate neurotransmitter receptor modulators being the more potent without noticeable untoward effects on the animals' wellbeing (Study 3). Specifically, the SuMN GABA activation results in increased body weight gain,

Fig. 7. SuMN inhibition with Triple Cocktail (TC) induces obesity and insulin resistance in rats fed regular chow. Rats fed regular chow were continuously infused with vehicle or TC (Muscimol/CNQX/dAP5, 3.6/1.8/120 nmol/day) at the medial SuMN area for four weeks. Compared with vehicle group, TC increased GTT insulin AUC (163%, $p = 0.009$) (C, D) but not glucose AUC (A, B) with a resultant reduction in Belfiore insulin sensitivity index (42%, $p = 0.028$) (E). Such treatment also increased the body weight gain by 2.3 fold (21% increase vs 9% increase in vehicle group, $p < 0.0001$) (F, G) and white adipose tissue (WAT) weight (parametrial pWAT by 117%, $p < 0.0001$; retroperitoneal rWAT by 85%, $p = 0.0004$ and total tl WAT by 107%, $p < 0.0001$) (H) compared to vehicle group. TC-treated rats consumed 21% more food than vehicle rats ($p < 0.0001$) (I, J) and had an increased feed efficiency relative to vehicle control (85%, $p < 0.0001$) (K). Such TC treatment also increased plasma glucose (8%, $p = 0.008$) (L), insulin (123%, $p = 0.0004$) (M) and HOMA-IR (145%, $p < 0.0004$) (N) as well as plasma leptin (126%, $p = 0.004$) (O) and liver triglyceride (55%, $p = 0.002$) (P). The relative basal oxygen consumption rate (OCR) of pWAT was reduced by 42% ($p = 0.004$) by TC relative to control (Q). *Significance, $p < 0.05$.

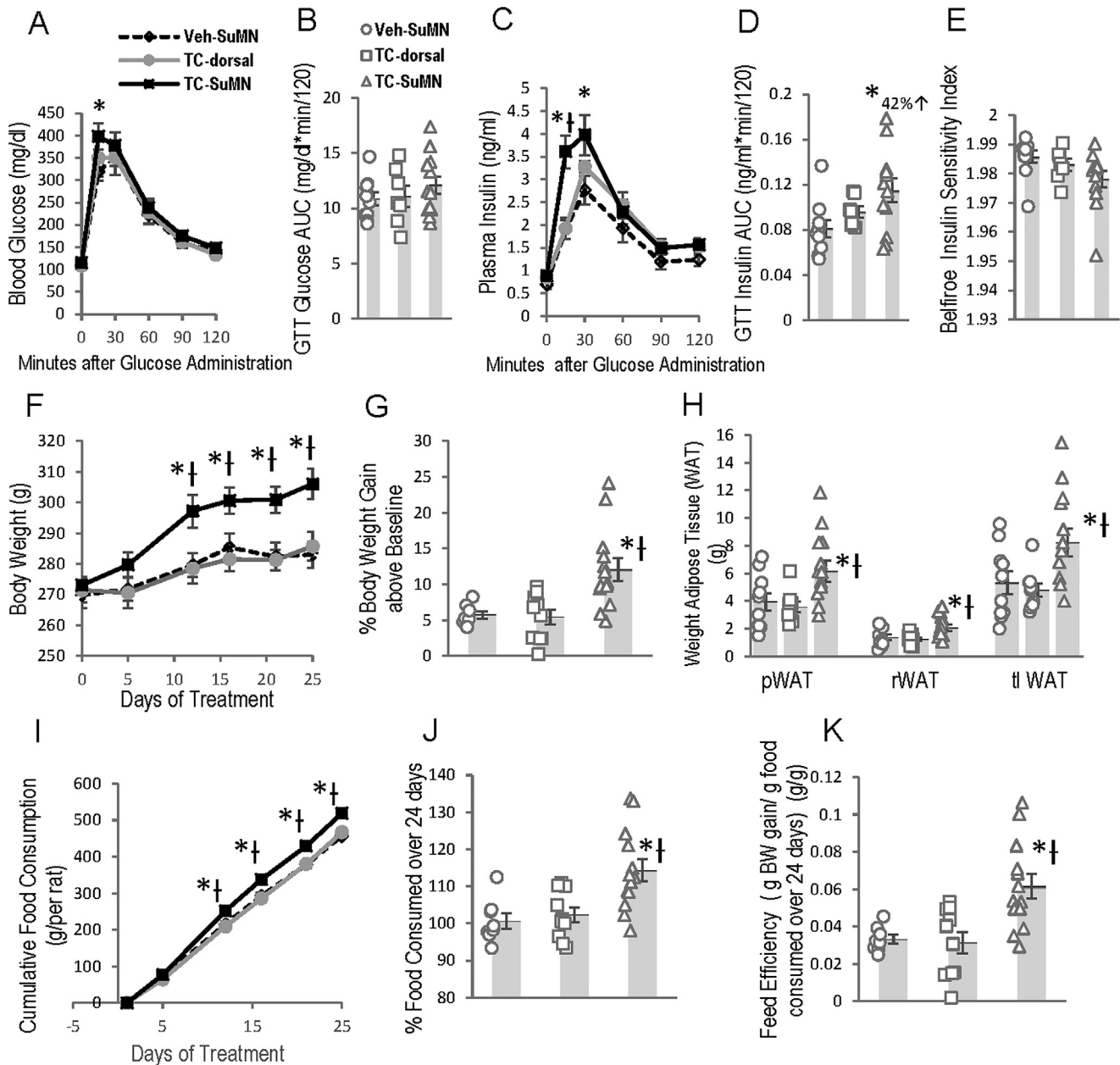
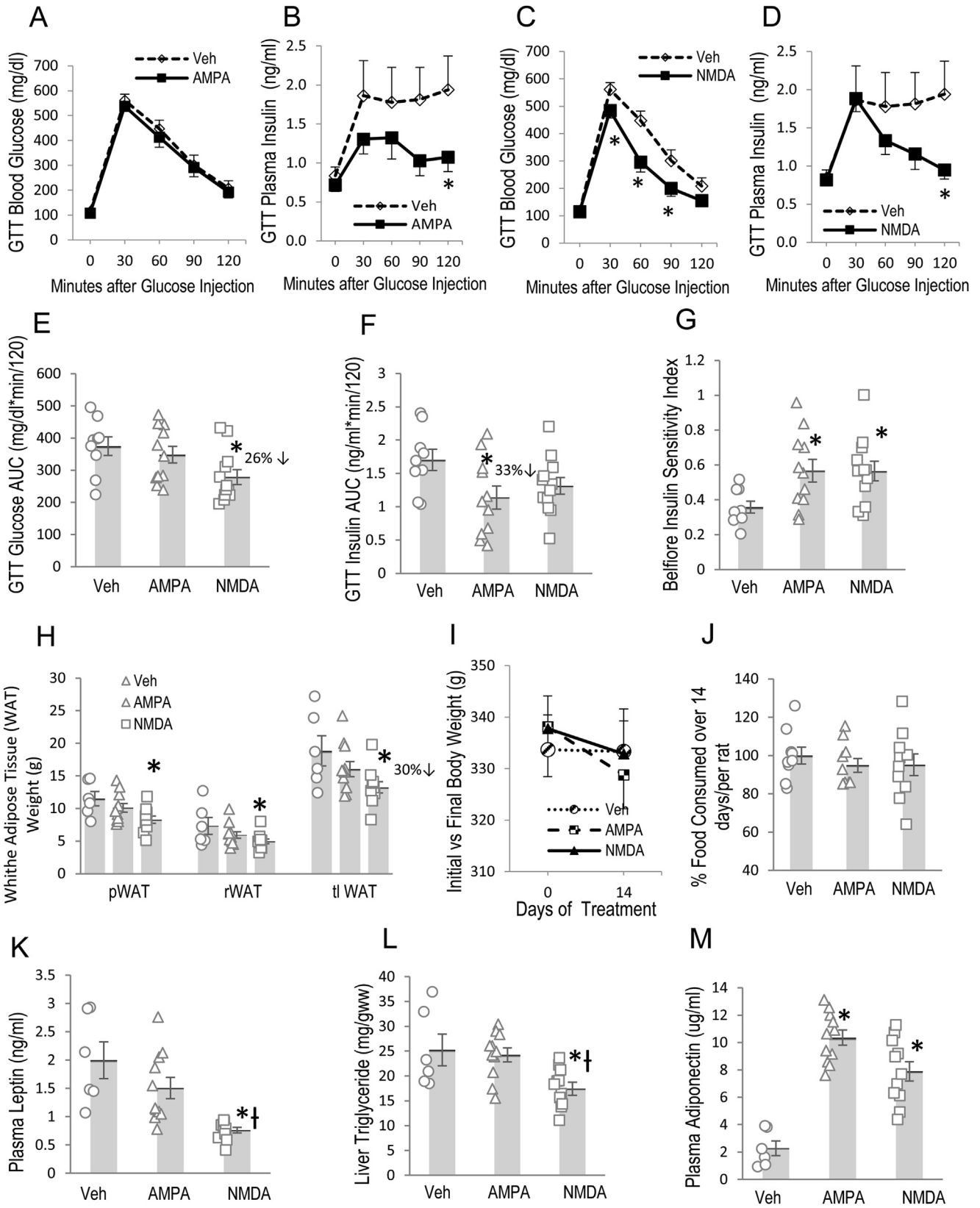


Fig. 8. Lack of metabolic effect of Triple Cocktail (TC) infused at 1.5 mm dorsal to the medial SuMN. Rats fed regular chow were divided into 3 groups and continuously infused for three weeks with vehicle at medial SuMN area, TC (Muscimol/CNQX/dAP5, 3.6/1.8/12 nmol/day) at the medial SuMN area or TC at an area 1.5 mm dorsal to the medial SuMN. Compared with vehicle, TC at medial SuMN area (TC-SuMN) but not at an area 1.5 mm dorsal to the SuMN (TC-dorsal) increased GTT insulin AUC (42%, $p = 0.021$) (C, D) without a change in glucose AUC (A, B) with a resultant reduction in Belfiore insulin sensitivity index (0.4%, $p = 0.05$) (E). TC-SuMN but not TC-dorsal treatment increased % body weight gain by 2.1 fold (12% vs 5.7% increase in vehicle group, $p = 0.006$) (F, G) and white adipose tissue (WAT) weight (parametrial pWAT by 57%, $p = 0.017$; retroperitoneal rWAT by 52%, $p = 0.03$; and total tWAT by 56%, $p = 0.018$) (H). The TC-SuMN but not TC-dorsal treated rats consumed 14% more food than vehicle rats ($p = 0.004$) (I, J) and had an increased feed efficiency relative to vehicle control (85%, $p = 0.004$) (K). Compared with TC-dorsal infused rats, TC-SuMN infused rats significantly increased %body weight gain by 2.2 fold (12% vs 5.5% increase in TC-dorsal group, $p = 0.004$) (F, G), WAT weight (pWAT by 73%, $p = 0.016$; rWAT by 69%, $p = 0.018$; tWAT by 72%, $p = 0.015$) (H), food consumption (12%, $p = 0.006$) (I, J) and feed efficiency (96%, $p = 0.003$) (K). *Significance vs Veh-SuMN, $p < 0.05$; †Significance vs TC-dorsal, $p < 0.05$.

feed efficiency and fasting plasma insulin without influencing fasting plasma glucose. This suggests that SuMN GABA activation mobilizes neuronal circuits involved in feeding and insulin secretion/sensitivity regulation (e.g., the striatum, the arcuate nucleus of the hypothalamus) but not in regulating hepatic glucose output, a primary source of fasting plasma glucose.

Juxtaposed to this response is the case for glutamate receptors blockade that appears to influence hepatic glucose production regulating centers (e.g., the paraventricular nucleus). However, when both receptor manipulations are made a broad spectrum of metabolic syndrome is achieved. These findings highlight potential neurophysiological differences between inhibition of



SuMN activity via GABA activation versus blockade of glutamate stimulation. We therefore employed the combination of GABA_A agonist and AMPA antagonist (SuMNI-DC) or GABA_A agonist and AMPA plus NMDA antagonists (SuMNI-TC) to inhibit the neuronal activity at the medial SuMN area in our subsequent studies of SuMN area regulation of metabolism. Secondly, SuMNI-DC treatment was sufficient to induce insulin resistance (in both HFD-resistant rats fed HFD and HFD-sensitive rats fed regular chow), without significant increase of feeding, body weight or body fat during the 3-week study period (Studies 4A and 5A) suggesting a direct effect of such treatment on neuroendocrine modulation of peripheral insulin action. Thirdly, the effect of SuMNI-TC (adding NMDA receptor antagonist to DC) infusion did result in increased feeding as well as increased feed efficiency (either due to decreased energy expenditure and/or channeling of substrates and calories preferentially into lipid stores) that each could consequently potentiate the observed body weight and body fat store gain during the 2–4 week study periods. The increased feeding effect alone of SuMNI-TC treatment is not sufficient to account for the increase in body weight or fat and does not itself impact feeding efficiency. The permissive role of NMDA receptor blockade of SuMN neuronal activity within a SuMNI-DC (GABA_A agonist/AMPA antagonist) background on body fat gain is consistent with the observed effect of NMDA receptor agonist stimulation of SuMN neuronal activity to reduce body fat stores, plasma leptin, and glucose intolerance and increase plasma adiponectin in obese HFD sensitive rats (and so to a much greater degree than AMPA receptor stimulation) (Study 7). Potential mechanisms for the prominent role of NMDA receptor ligands in metabolic regulation may relate to observations that glutamate NMDA receptor stimulation induces phasic neuronal firing that can be more efficient to increase neurotransmitter level at neuronal terminal regions than glutamate AMPA receptor stimulation which induces tonic neuronal firing (Chergui et al., 1993; Zakharov et al., 2016; Zweifel et al., 2009).

Respecting the influence of the SuMNI-TC to stimulate food consumption, it is relevant that the SuMN is functionally linked to the VTA-striatum dopamine reward system (a central part of the mesolimbic system regulating feeding). The intra-SuMN self-administration of AMPA or GABA_A receptor antagonist is associated with dopamine release in the striatal nucleus accumbens (Ikemoto, 2005; Ikemoto et al., 2004), part

of the molecular signal mechanism for (feeding) reward fulfillment at this site. Moreover, intracranial reinforcing treatments that activate the mesolimbic dopamine system also activate the SuMN as revealed by a marked increase in c-Fos expression therein (Arvanitogiannis et al., 1997; Ikemoto et al., 2003). Decreased SuMN activity may reduce striatal nucleus accumbens dopaminergic signaling leading to overfeeding. Low dopamine function in the mesolimbic reward system (decreases in dopamine D2 receptors and in dopamine release) is observed and operative in obesity and metabolic syndrome (Fulton et al., 2006; Geiger et al., 2009; Wang et al., 2001) due in part to food overconsumption as a means to compensate for the weak dopamine reward signal (Stice et al., 2008). Although direct neuroanatomical connections from the SuMN to the VTA-nucleus accumbens are scarce, the SuMN could indirectly modulate VTA dopamine neurons via relay nuclei with which it communicates such as the lateral and medial septum, medial preoptic area and in particular the lateral hypothalamus (LH) (directly and via the lateral septum) which all project densely to the VTA and regulate dopamine-mediated feeding and motivated behaviors (Godfrey and Borgland, 2019; Ikemoto, 2010; Kalló et al., 2015; Luo et al., 2011; Pan and McNaughton, 2004; Tyree and de Lecea, 2017). The SuMN is also neuro-anatomically connected with the lateral habenula nucleus (LHb) and the laterodorsal tegmental nucleus (LDTg) whose activation is known to modulate midbrain dopamine neurons and food intake (Coimbra et al., 2019; Hong et al., 2011; Lodge and Grace, 2006; Reiner et al., 2018; Stamatakis et al., 2016). Collectively, activation of the SuMN could via these above stated neuronal pathways stimulate dopamine release within the mesolimbic system to elicit motivation/reward/satiety signals and subsequent cessation of the feeding bout. Thus, the increase in feeding induced by SuMNI-TC could result from alteration (inhibition) of the brain (dopamine) reward and arousal systems. An additional prominent efferent target of the SuMN that regulates feeding behavior is the hippocampus. The hippocampus is not only central to memory, but also is involved in regulation of feeding behaviors (Davidson et al., 2009; Forloni et al., 1986). The hippocampus can detect interoceptive signals of hunger and satiety and forms memory of a meal to inhibit subsequent food intake in humans (Coppin, 2016; Higgs, 2016). It is thus possible that SuMNI-TC compromised hippocampal learning-conditioning in food intake control. Finally, it must be reiterated that the increase in food consumption with the SuMNI-TC treatment is not great

Fig. 9. Circadian-timed stimulation of the medial SuMN area with AMPA or NMDA improved HFD-induced metabolic syndrome. HFD-sensitive rats were fed HFD for three months and then received 1 minute intra-SuMN infusion (0.5 μ l) of vehicle (Veh), AMPA (30 pmol in 0.5 μ l) or NMDA/*D*-serine (250/250 pmol in 0.5 μ l) starting one hour before light offset (ZT13) daily for two weeks. Compared with vehicle, AMPA decreased GTT insulin AUC by 33% ($p = 0.031$) (B, F) with no change in glucose AUC (A, E). NMDA/*D*-serine decreased GTT glucose AUC by 26% ($p = 0.016$) (C, E) with no significant reduction in insulin AUC (23%, $p = 0.065$) (D, F). As a result, AMPA and NMDA/*D*-serine treatments increased Before insulin sensitivity index by 58% ($p = 0.016$) and 58% ($p = 0.009$) respectively (G). Compared with vehicle, NMDA/*D*-serine treatment reduced white adipose tissue (WAT) weight (parametrial pWAT by 28%, $p = 0.01$; retroperitoneal rWAT by 33%, $p = 0.041$; total tl WAT by 30%, $p = 0.015$) (H) while not changing body weight (I) and food consumption (J). NMDA/*D*-serine also reduced plasma leptin (62%, $p = 0.0001$) (K) and liver triglyceride (31%, $p = 0.016$) (L). Both AMPA and NMDA/*D*-serine treatments increased plasma adiponectin by 355% ($p < 0.0001$) and 247% ($p = 0.0001$) respectively (M). Compared with AMPA, NMDA treatment reduced plasma leptin (49%, $p = 0.001$) (K) and liver triglyceride (28%, $p = 0.002$) (L) *Significance vs vehicle, $p < 0.05$, [†]Significance vs AMPA, $p < 0.05$.

enough to explain the induction of metabolic syndrome and obesity in these animals.

In addition to its connections to multiple feeding, reward and emotion regulation centers in the brain as described above, the SuMN also communicates with other brain centers that regulate metabolism independent of feeding. Among such centers, importantly the SuMN sends efferent connections directly and indirectly to the SCN, the biological clock pacemaker region for integration of biological circadian rhythms throughout the body, including those of fuel metabolism (Bass and Takahashi, 2010; Ding et al., 2018; Luo et al., 2018). Dopaminergic neurons within the medial SuMN project directly to the SCN region where the circadian peak of such input potentiates the insulin sensitive, lean condition (Luo et al., 2018). Thus, the DC or TC inhibition of medial SuMN neuronal activity (including dopaminergic activity therein) could reduce circadian dopamine release at the SCN clock region to manifest the insulin resistant state as observed herein. In addition, the medial SuMN could also indirectly modulate clock function via its dopaminergic projections to the lateral septum and medial preoptic area both of which communicate strongly to the SCN (Krout et al., 2002; Miller and Lonstein, 2009). Furthermore, in seasonal animals, the acrophase relationship of dopaminergic circadian activity at the SCN region with respect to that of serotonergic activity at the SCN has been observed to modulate peripheral seasonal metabolic status (obese, insulin resistant [e.g., winter] vs lean, insulin sensitive [e.g., summer]) as a function of the changing seasonal inter-acrophase time relation (i.e., time between each circadian peak activity) (Meier and Cincotta, 1996) and the SuMN communicates with the raphe nuclei that provide serotonergic projections to the SCN (Glass et al., 2003; Morin, 1999). Therefore, the SuMN could also participate in coordinating the circadian activities of both serotonin and dopamine at the clock region to regulate peripheral fuel metabolism.

The increase in body weight gain induced by SuMNI-TC is accompanied by a moderate increase in food consumption coupled to a marked increase in feed efficiency (grams of body weight gain per gram of food consumed) (111% in Fig. 5K [HFD] and 85% in Fig. 7K [regular chow]) and body fat store level (72% in Fig. 5H [HFD] and 107% in Fig. 7H [regular chow]) indicating that the SuMNI induces a shift in energy balance in favor of fat storage. Animals treated with the SuMNI-TC had not only increased white adipose tissue mass but also a reduced adipocyte basal oxygen consumption rate (Fig. 7Q). Since the adipocyte fatty acid oxidation rate was unaltered by such treatment, these findings suggest a reduced oxidation of glucose, consistent with the observed insulin resistance and glucose intolerance and supportive of glucose channeled towards hyperinsulinemia-stimulated lipogenesis (Denton et al., 1977; Gandemer et al., 1983). Moreover, SuMNI-TC also increased liver triglyceride content again suggestive of hyperinsulinemia-stimulated lipid synthesis. The increased fat mass of SuMNI-TC treated animals was associated with hyperleptinemia and hyperinsulinemia,

factors that potentiate insulin and leptin resistance in the brain and peripheral organs (e.g., liver, adipose and muscle) (Konner and Bruning, 2012; Stern et al., 2016; Yadav et al., 2013) consistent with the findings of SuMNI-induced obesity and insulin resistance state in this study. Also consistent with the observed insulin resistant state in SuMNI animals is the concurrent presence of hyperinsulinemia and increased hepatic gluconeogenesis and hepatic glucose output (assessed via the pyruvate tolerance test) (Fig. 4F).

Collectively, these findings indicate that the circadian GABA/glutamate input balance at the medial SuMN area could serve as a molecular neuronal switch controlling its communication to target neuronal circuits to support energy conservation or utilization dependent upon the (circadian) activation (increased glutamate to GABA input) or inhibition (increased GABA to glutamate input) state of the medial SuMN area. Many SuMN-projecting brain regions known to actively participate in the regulation of peripheral fuel metabolism express glutamate and/or GABA (e.g., VMH, lateral habenula, lateral dorsal tegmental nucleus, septum, preoptic area, lateral hypothalamus, raphe nuclei) (Brinshaw et al., 2010; Bueno et al., 2019; Mickelsen et al., 2019; Monti, 2010; Tong et al., 2007), and some are suggested to contribute to glutamate and GABA signaling at the SuMN (Gonzalo-Ruiz et al., 1999; Kiss et al., 2002; Leranth et al., 1999a, 1999b). Furthermore, GABA and glutamate could be locally released as neurons with singular glutamatergic, GABAergic and dual glutamatergic/GABAergic neurotransmitter phenotypes have been identified in the SuMN (Hashimoto et al., 2018; Root et al., 2018). Thus, the present findings support that the excitatory glutamate and inhibitory GABA signaling from multiple metabolically relevant brain centers are somehow integrated at the SuMN area and the net balance of these GABAergic /glutamatergic inputs at the medial SuMN area with respect to a particular circadian time in turn determines its functional output to control energy balance.

The limitations of this study include the lack of identification of which type of neurons within the SuMN are responding to the GABA and glutamate receptor ligands employed, the absence of a time course of changes in metabolic events during the treatment period, lack of assessment of whole body metabolic rate and fuel utilization/production parameters (i.e., whole body protein turnover, FFA oxidation, and lipid synthesis rates), and the long term metabolic influence of such treatment (of note, we observed a slowing of body weight gain towards the end of the 2-week TC infusion period while subsequent replacement of the osmotic pump filled with fresh TC maintained the steady increase in body weight [Fig. 7F]). However, now having the present findings in hand such future studies are warranted. Moreover, the current findings evoke the value of further studies to elucidate the intricate connections of this SuMN neuronal circuitry involved in peripheral metabolism, feeding behavior, and energy balance regulation. For instance, it would be important to understand the relation between SuMN GABA and glutamate receptor activation and the recently identified

SuMN ghrelin and GLP-1 receptor mediated regulation of feeding (Le May et al., 2019; Lopez-Ferreras et al., 2019; Vogel et al., 2016).

In conclusion, chronic inhibition of neuronal activity at the medial SuMN area via direct local GABA receptor agonist plus NMDA and AMPA glutamate receptor antagonists (TC) infusion, facilitates the hyperinsulinemia, insulin resistant, obese condition characterized by increased food consumption, increased feed efficiency, hyperleptinemia, and increased liver fat in both animals fed regular chow diet and in animals fed a high fat diet that are resistant to its obesogenic effects. Such treatment with only GABA agonist plus AMPA antagonist (DC) is sufficient to induce insulin resistance in these model systems without significant alteration of feeding or body composition during the period examined. Additionally, among animals fed a high fat diet that are resistant to its obesogenic effects, inhibition of the medial SuMN area with either the DC or TC induces frank glucose intolerance. Consistent with such findings, circadian-timed activation of neuronal activity at the medial SuMN area with direct local infusion of either AMPA or NMDA receptor agonist at the onset of nocturnal locomotor activity ameliorates insulin resistance in high fat diet fed animals sensitive to its obesogenic effects. The metabolic syndrome is a complex disorder associated with functional alterations of multiple brain systems, in particular disrupted circadian rhythmicity (Branecky et al., 2015; Kohsaka et al., 2007), altered motivation-reward regulation (Kenny, 2011; Rada et al., 2010) and impaired learning/memory (Davidson et al., 2013; Kumari et al., 2000). The SuMN comprises an integral node within brain neuronal circuits implicated in the regulation of arousal/sleep, motivation/reward, and learning/memory (Ikemoto, 2010; Pan and McNaughton, 1997; Pedersen et al., 2017) with a unique efferent connection to the circadian clock (SCN) through its dopaminergic innervation (Luo et al., 2018). The present study findings demonstrate that the medial SuMN area in the posterior hypothalamus regulates energy metabolism and feeding as a function of its (circadian) net GABA versus glutamate receptor activation ratio with net neuronal inhibition facilitating metabolic syndrome and net circadian-timed stimulation ameliorating or preventing metabolic syndrome. Identification of the medial SuMN area as a novel hypothalamic metabolic control structure provides new insights to the complex brain neuronal mechanisms linking feeding and non-feeding related mechanisms underlying the development of obesity and obesity-associated metabolic syndrome.

CONFLICT OF INTEREST STATEMENT

The authors are current or former employees of VeroScience LLC. The authors declare that they have no competing interests.

ACKNOWLEDGEMENTS

The authors are grateful to Yelena Trubitsyna for her excellent technical assistance.

AUTHOR CONTRIBUTIONS

Y. Z. and A.H.C. designed, discussed and wrote the manuscript. Y. Z., C.S., M.E. and T. T. performed the experiments and analyzed the data.

FUNDING

This study was funded by VeroScience LLC of Tiverton, RI and S2 Therapeutics of Bristol, TN.

REFERENCES

- Allen TA, Narayanan NS, Kholodar-Smith DB, Zhao Y, Laubach M, Brown TH (2008) Imaging the spread of reversible brain inactivations using fluorescent muscimol. *J Neurosci Methods* 171:30–38.
- Arvanitogiannis A, Flores C, Shizgal P (1997) Fos-like immunoreactivity in the caudal diencephalon and brainstem following lateral hypothalamic self-stimulation. *Behav Brain Res* 88:275–279.
- Bass J, Takahashi JS (2010) Circadian integration of metabolism and energetics. *Science* 330:1349–1354.
- Berridge KC, Ho CY, Richard JM, DiFeliceantonio AG (2010) The tempted brain eats: pleasure and desire circuits in obesity and eating disorders. *Brain Res* 1350:43–64.
- Branecky KL, Niswender KD, Pendergast JS (2015) Disruption of daily rhythms by high-fat diet is reversible. *PLoS One* 10:e0137970.
- Brinschwitz K, Dittgen A, Madai VI, Lommel R, Geisler S, Veh RW (2010) Glutamatergic axons from the lateral habenula mainly terminate on GABAergic neurons of the ventral midbrain. *Neuroscience* 168:463–476.
- Broadbent NJ, Squire LR, Clark RE (2010) Sustained dorsal hippocampal activity is not obligatory for either the maintenance or retrieval of long-term spatial memory. *Hippocampus* 20:1366–1375.
- Bueno D, Lima LB, Souza R, Goncalves L, Leite F, Souza S, Furigo IC, Donato Jr J, et al. (2019) Connections of the laterodorsal tegmental nucleus with the habenular-interpeduncular-raphe system. *J Comp Neurol* 527:3046–3072.
- Castillo-Ruiz A, Gall AJ, Smale L, Nunez AA (2013) Day-night differences in neural activation in histaminergic and serotonergic areas with putative projections to the cerebrospinal fluid in a diurnal brain. *Neuroscience* 250:352–363.
- Chang S, Graham B, Yakubu F, Lin D, Peters JC, Hill JO (1990) Metabolic differences between obesity-prone and obesity-resistant rats. *Am J Physiol* 259:R1103–1110.
- Chergui K, Charlety PJ, Akaoka H, Saunier CF, Brunet JL, Buda M, Svensson TH, Chouvet G (1993) Tonic activation of NMDA receptors causes spontaneous burst discharge of rat midbrain dopamine neurons in vivo. *Eur J Neurosci* 5:137–144.
- Cincotta AH, Schiller BC, Landry RJ, Herbert SJ, Miers WR, Meier AH (1993) Circadian neuroendocrine role in age-related changes in body fat stores and insulin sensitivity of the male Sprague-Dawley rat. *Chronobiol Int* 10:244–258.
- Coimbra B, Soares-Cunha C, Vasconcelos NAP, Domingues AV, Borges S, Sousa N, Rodrigues AJ (2019) Role of laterodorsal tegmentum projections to nucleus accumbens in reward-related behaviors. *Nat Commun* 10:4138.
- Coppin G (2016) The anterior medial temporal lobes: Their role in food intake and body weight regulation. *Physiol Behav* 167:60–70.
- Davidson TL, Chan K, Jarrard LE, Kanoski SE, Clegg DJ, Benoit SC (2009) Contributions of the hippocampus and medial prefrontal cortex to energy and body weight regulation. *Hippocampus* 19:235–252.
- Davidson TL, Hargrave SL, Swithers SE, Sample CH, Fu X, Kinzig KP, Zheng W (2013) Inter-relationships among diet, obesity and

- hippocampal-dependent cognitive function. *Neuroscience* 253:110–122.
- Davis S, Butcher SP, Morris RG (1992) The NMDA receptor antagonist D-2-amino-5-phosphonopentanoate (D-AP5) impairs spatial learning and LTP in vivo at intracerebral concentrations comparable to those that block LTP in vitro. *J Neurosci* 12:21–34.
- Denton R, Bridges B, Brownsey R, Evans G, Hughes W, Stansbie D (1977) Regulation of the conversion of glucose into fat in white adipose tissue by insulin [proceedings]. *Biochem Soc Trans* 5:894–900.
- Ding G, Gong Y, Eckel-Mahan KL, Sun Z (2018) Central Circadian clock regulates energy metabolism. *Adv Exp Med Biol* 1090:79–103.
- Dourmashkin JT, Chang GQ, Hill JO, Gayles EC, Fried SK, Leibowitz SF (2006) Model for predicting and phenotyping at normal weight the long-term propensity for obesity in Sprague-Dawley rats. *Physiol Behav* 87:666–678.
- Egecioglu E, Skibicka KP, Hansson C, Alvarez-Crespo M, Friberg PA, Jerlhag E, Engel JA, Dickson SL (2011) Hedonic and incentive signals for body weight control. *Rev Endocr Metab Disord* 12:141–151.
- Ferrario CR, Labouebe G, Liu S, Nieh EH, Routh VH, Xu S, O'Connor EC (2016) Homeostasis meets motivation in the battle to control food intake. *J Neurosci* 36:11469–11481.
- Forloni G, Fisone G, Guitani A, Ladinsky H, Consolo S (1986) Role of the hippocampus in the sex-dependent regulation of eating behavior: studies with kainic acid. *Physiol Behav* 38:321–326.
- Fulton S, Pissios P, Manchon RP, Stiles L, Frank L, Pothos EN, Maratos-Flier E, Flier JS (2006) Leptin regulation of the mesoaccumbens dopamine pathway. *Neuron* 51:811–822.
- Gandemer G, Durand G, Pascal G (1983) Relative contribution of the main tissues and organs to body fatty acid synthesis in the rat. *Lipids* 18:223–228.
- Geiger BM, Haburcak M, Avena NM, Moyer MC, Hoebel BG, Pothos EN (2009) Deficits of mesolimbic dopamine neurotransmission in rat dietary obesity. *Neuroscience* 159:1193–1199.
- Glass JD, Grossman GH, Farnbauch L, DiNardo L (2003) Midbrain raphe modulation of nonphotic circadian clock resetting and 5-HT release in the mammalian suprachiasmatic nucleus. *J Neurosci* 23:7451–7460.
- Gliddon CM, Darlington CL, Smith PF (2005) Effects of chronic infusion of a GABAA receptor agonist or antagonist into the vestibular nuclear complex on vestibular compensation in the guinea pig. *J Pharmacol Exp Ther* 313:1126–1135.
- Godfrey N, Borgland SL (2019) Diversity in the lateral hypothalamic input to the ventral tegmental area. *Neuropharmacology* 154:4–12.
- Gonzalo-Ruiz A, Morte L, Flecha JM, Sanz JM (1999) Neurotransmitter characteristics of neurons projecting to the supramammillary nucleus of the rat. *Anat Embryol (Berl)* 200:377–392.
- Goodman MN, Druz SM, McElaney MA, Belur E, Ruderman NB (1983) Glucose uptake and insulin sensitivity in rat muscle: changes during 3–96 weeks of age. *Am J Physiol* 244:E93–100.
- Hashimoto-dani Y, Karube F, Yanagawa Y, Fujiyama F, Kano M (2018) Supramammillary nucleus afferents to the dentate gyrus co-release glutamate and GABA and potentiate granule cell output. *Cell Rep* 25(2704–2715) e2704.
- Hayakawa T, Ito H, Zyo K (1993) Neuroanatomical study of afferent projections to the supramammillary nucleus of the rat. *Anat Embryol (Berl)* 188:139–148.
- Higgs S (2016) Cognitive processing of food rewards. *Appetite* 104:10–17.
- Hong S, Zhou TC, Smith M, Saleem KS, Hikosaka O (2011) Negative reward signals from the lateral habenula to dopamine neurons are mediated by rostromedial tegmental nucleus in primates. *J Neurosci* 31:11457–11471.
- Ikemoto S (2004) Unconditional hyperactivity and transient reinforcing effects of NMDA administration into the ventral tegmental area in rats. *Psychopharmacology (Berl)* 172:202–210.
- Ikemoto S (2005) The supramammillary nucleus mediates primary reinforcement via GABA(A) receptors. *Neuropsychopharmacology* 30:1088–1095.
- Ikemoto S (2010) Brain reward circuitry beyond the mesolimbic dopamine system: a neurobiological theory. *Neurosci Biobehav Rev* 35:129–150.
- Ikemoto S, Witkin BM, Morales M (2003) Rewarding injections of the cholinergic agonist carbachol into the ventral tegmental area induce locomotion and c-Fos expression in the retrosplenial area and supramammillary nucleus. *Brain Res* 969:78–87.
- Ikemoto S, Witkin BM, Zangen A, Wise RA (2004) Rewarding effects of AMPA administration into the supramammillary or posterior hypothalamic nuclei but not the ventral tegmental area. *J Neurosci* 24:5758–5765.
- Johnson AW (2013) Eating beyond metabolic need: how environmental cues influence feeding behavior. *Trends Neurosci* 36:101–109.
- Kallo I, Molnar CS, Szoke S, Fekete C, Hrabovszky E, Liposits Z (2015) Area-specific analysis of the distribution of hypothalamic neurons projecting to the rat ventral tegmental area, with special reference to the GABAergic and glutamatergic efferents. *Front Neuroanat* 9:112.
- Kenny PJ (2011) Reward mechanisms in obesity: new insights and future directions. *Neuron* 69:664–679.
- Kimbro JR, Kelly PJ, Drummond JC, Cole DJ, Patel PM (2000) Isoflurane and pentobarbital reduce AMPA toxicity in vivo in the rat cerebral cortex. *Anesthesiology* 92:806–812.
- Kiss J, Csaki A, Bokor H, Kocsis K, Kocsis B (2002) Possible glutamatergic/aspartatergic projections to the supramammillary nucleus and their origins in the rat studied by selective [(3)H]D-aspartate labelling and immunocytochemistry. *Neuroscience* 111:671–691.
- Kohsaka A, Laposky AD, Ramsey KM, Estrada C, Joshu C, Kobayashi Y, Turek FW, Bass J (2007) High-fat diet disrupts behavioral and molecular circadian rhythms in mice. *Cell Metab* 6:414–421.
- Konner AC, Bruning JC (2012) Selective insulin and leptin resistance in metabolic disorders. *Cell Metab* 16:144–152.
- Kretschmer BD (1999) Modulation of the mesolimbic dopamine system by glutamate: role of NMDA receptors. *J Neurochem* 73:839–848.
- Krout KE, Kawano J, Mettenleiter TC, Loewy AD (2002) CNS inputs to the suprachiasmatic nucleus of the rat. *Neuroscience* 110:73–92.
- Kumari M, Brunner E, Fuhrer R (2000) Minireview: mechanisms by which the metabolic syndrome and diabetes impair memory. *J Gerontol A Biol Sci Med Sci* 55:B228–232.
- Le May MV, Hume C, Sabatier N, Schele E, Bake T, Bergstrom U, Menzies J, Dickson SL (2019) Activation of the rat hypothalamic supramammillary nucleus by food anticipation, food restriction or ghrelin administration. *J Neuroendocrinol* 31 e12676.
- Leranth C, Carpi D, Buzsaki G, Kiss J (1999a) The entorhino-septo-supramammillary nucleus connection in the rat: morphological basis of a feedback mechanism regulating hippocampal theta rhythm. *Neuroscience* 88:701–718.
- Leranth C, Shanabrough M, Horvath TL (1999b) Estrogen receptor-alpha in the raphe serotonergic and supramammillary area calretinin-containing neurons of the female rat. *Exp Brain Res* 128:417–420.
- Lodge DJ, Grace AA (2006) The laterodorsal tegmentum is essential for burst firing of ventral tegmental area dopamine neurons. *Proc Natl Acad Sci U S A* 103:5167–5172.
- Lopez-Ferreras L, Eerola K, Mishra D, Shevchouk OT, Richard JE, Nilsson FH, Hayes MR, Skibicka KP (2019) GLP-1 modulates the supramammillary nucleus-lateral hypothalamic neurocircuit to control ingestive and motivated behavior in a sex divergent manner. *Mol Metab* 20:178–193.
- Luo AH, Tahsili-Fahadan P, Wise RA, Lupica CR, Aston-Jones G (2011) Linking context with reward: a functional circuit from hippocampal CA3 to ventral tegmental area. *Science* 333:353–357.

- Luo S, Zhang Y, Ezrokhi M, Li Y, Tsai TH, Cincotta AH (2018) Circadian peak dopaminergic activity response at the biological clock pacemaker (suprachiasmatic nucleus) area mediates the metabolic responsiveness to a high-fat diet. *J Neuroendocrinol* 30.
- Lutz TA (2012) Effects of amylin on eating and adiposity. *Handb Exp Pharmacol*:231–250.
- Maalouf M, Dykes RW, Miasnikov AA (1998) Effects of D-AP5 and NMDA microiontophoresis on associative learning in the barrel cortex of awake rats. *Brain Res* 793:149–168.
- Meier AH, Cincotta AH (1996) Circadian rhythms regulate the expression of the thrifty genotype/phenotype. *Diabetes Reviews* 4.
- Mickelsen LE, Bolisetty M, Chimileski BR, Fujita A, Beltrami EJ, Costanzo JT, Naparstek JR, Robson P, et al. (2019) Single-cell transcriptomic analysis of the lateral hypothalamic area reveals molecularly distinct populations of inhibitory and excitatory neurons. *Nat Neurosci* 22:642–656.
- Miller SM, Lonstein JS (2009) Dopaminergic projections to the medial preoptic area of postpartum rats. *Neuroscience* 159:1384–1396.
- Monti JM (2010) The role of dorsal raphe nucleus serotonergic and non-serotonergic neurons, and of their receptors, in regulating waking and rapid eye movement (REM) sleep. *Sleep Med Rev* 14:319–327.
- Morin LP (1999) Serotonin and the regulation of mammalian circadian rhythmicity. *Ann Med* 31:12–33.
- Morris RG, Steele RJ, Bell JE, Martin SJ (2013) N-methyl-d-aspartate receptors, learning and memory: chronic intraventricular infusion of the NMDA receptor antagonist d-AP5 interacts directly with the neural mechanisms of spatial learning. *Eur J Neurosci* 37:700–717.
- Nicolelis NAL (1999) *Methods for neural ensemble recordings*. CRC Press LLC.
- Pan WX, McNaughton N (1997) The medial supramammillary nucleus, spatial learning and the frequency of hippocampal theta activity. *Brain Res* 764:101–108.
- Pan WX, McNaughton N (2002) The role of the medial supramammillary nucleus in the control of hippocampal theta activity and behaviour in rats. *Eur J Neurosci* 16:1797–1809.
- Pan WX, McNaughton N (2004) The supramammillary area: its organization, functions and relationship to the hippocampus. *Prog Neurobiol* 74:127–166.
- Pedersen NP, Ferrari L, Venner A, Wang JL, Abbott SGB, Vujovic N, Arrigoni E, Saper CB, et al. (2017) Supramammillary glutamate neurons are a key node of the arousal system. *Nat Commun* 8:1405.
- Plaisier F, Hume C, Menzies J (2020) Neural connectivity between the hypothalamic supramammillary nucleus and appetite- and motivation-related regions of the rat brain. *J Neuroendocrinol* 32 e12829.
- Rada P, Bocarsly ME, Barson JR, Hoebel BG, Leibowitz SF (2010) Reduced accumbens dopamine in Sprague-Dawley rats prone to overeating a fat-rich diet. *Physiol Behav* 101:394–400.
- Rambousek L, Kleteckova L, Kubesova A, Jirak D, Vales K, Fritschy JM (2016) Rat intra-hippocampal NMDA infusion induces cell-specific damage and changes in expression of NMDA and GABAA receptor subunits. *Neuropharmacology* 105:594–606.
- Reiner DJ, Leon RM, McGrath LE, Koch-Laskowski K, Hahn JD, Kanoski SE, Miettlicki-Baase EG, Hayes MR (2018) Glucagon-like peptide-1 receptor signaling in the lateral dorsal tegmental nucleus regulates energy balance. *Neuropsychopharmacology* 43:627–637.
- Risold PY, Swanson LW (1996) Structural evidence for functional domains in the rat hippocampus. *Science* 272:1484–1486.
- Root DH, Zhang S, Barker DJ, Miranda-Barrientos J, Liu B, Wang HL, Morales M (2018) Selective brain distribution and distinctive synaptic architecture of dual glutamatergic-GABAergic neurons. *Cell Rep* 23:3465–3479.
- Ruan M, Young CK, McNaughton N (2017) Bi-directional theta modulation between the septo-hippocampal system and the mammillary area in free-moving rats. *Front Neural Circuits* 11:62.
- Schwartz MW, Woods SC, Porte Jr D, Seeley RJ, Baskin DG (2000) Central nervous system control of food intake. *Nature* 404:661–671.
- Seoane-Collazo P, Ferno J, Gonzalez F, Dieguez C, Leis R, Nogueiras R, Lopez M (2015) Hypothalamic-autonomic control of energy homeostasis. *Endocrine* 50:276–291.
- Shabat-Simon M, Levy D, Amir A, Rehavi M, Zangen A (2008) Dissociation between rewarding and psychomotor effects of opiates: differential roles for glutamate receptors within anterior and posterior portions of the ventral tegmental area. *J Neurosci* 28:8406–8416.
- Shepard PD, Mihailoff GA, German DC (1988) Anatomical and electrophysiological characterization of presumed dopamine-containing neurons within the supramammillary region of the rat. *Brain Res Bull* 20:307–314.
- Soussi R, Zhang N, Tahtakran S, Houser CR, Esclapez M (2010) Heterogeneity of the supramammillary-hippocampal pathways: evidence for a unique GABAergic neurotransmitter phenotype and regional differences. *Eur J Neurosci* 32:771–785.
- Stagkourakis S, Spigolon G, Williams P, Protzmann J, Fisone G, Broberger C (2018) A neural network for intermale aggression to establish social hierarchy. *Nat Neurosci* 21:834–842.
- Stalnaker TA, Berridge CW (2003) AMPA receptor stimulation within the central nucleus of the amygdala elicits a differential activation of central dopaminergic systems. *Neuropsychopharmacology* 28:1923–1934.
- Stamatakis AM, Van Swieten M, Basiri ML, Blair GA, Kantak P, Stuber GD (2016) Lateral hypothalamic area glutamatergic neurons and their projections to the lateral habenula regulate feeding and reward. *J Neurosci* 36:302–311.
- Stern JH, Rutkowski JM, Scherer PE (2016) Adiponectin, leptin, and fatty acids in the maintenance of metabolic homeostasis through adipose tissue crosstalk. *Cell Metab* 23:770–784.
- Stice E, Spoor S, Bohon C, Small DM (2008) Relation between obesity and blunted striatal response to food is moderated by TaqIA A1 allele. *Science* 322:449–452.
- Swanson LW (1982) The projections of the ventral tegmental area and adjacent regions: a combined fluorescent retrograde tracer and immunofluorescence study in the rat. *Brain Res Bull* 9:321–353.
- Timper K, Bruning JC (2017) Hypothalamic circuits regulating appetite and energy homeostasis: pathways to obesity. *Dis Model Mech* 10:679–689.
- Tong Q, Ye C, McCrimmon RJ, Dhillon H, Choi B, Kramer MD, Yu J, Yang Z, et al. (2007) Synaptic glutamate release by ventromedial hypothalamic neurons is part of the neurocircuitry that prevents hypoglycemia. *Cell Metab* 5:383–393.
- Travagli RA, Hermann GE, Browning KN, Rogers RC (2006) Brainstem circuits regulating gastric function. *Annu Rev Physiol* 68:279–305.
- Tsanov M (2018) Differential and complementary roles of medial and lateral septum in the orchestration of limbic oscillations and signal integration. *Eur J Neurosci* 48:2783–2794.
- Tyree SM, de Lecea L (2017) Lateral hypothalamic control of the ventral tegmental area: reward evaluation and the driving of motivated behavior. *Front Syst Neurosci* 11:50.
- Uyama N, Geerts A, Reynaert H (2004) Neural connections between the hypothalamus and the liver. *Anat Rec A Discov Mol Cell Evol Biol* 280:808–820.
- Vertes RP (1992) PHA-L analysis of projections from the supramammillary nucleus in the rat. *J Comp Neurol* 326:595–622.
- Vertes RP (2015) Major diencephalic inputs to the hippocampus: supramammillary nucleus and nucleus reuniens. *Circuitry and function*. *Prog Brain Res* 219:121–144.
- Vogel H, Wolf S, Rabasa C, Rodriguez-Pacheco F, Babaei CS, Stober F, Goldschmidt J, DiMarchi RD, et al. (2016) GLP-1 and estrogen conjugate acts in the supramammillary nucleus to reduce food-reward and body weight. *Neuropharmacology* 110:396–406.
- Wang GJ, Volkow ND, Logan J, Pappas NR, Wong CT, Zhu W, Netusil N, Fowler JS (2001) Brain dopamine and obesity. *Lancet* 357:354–357.

Yadav A, Kataria MA, Saini V, Yadav A (2013) Role of leptin and adiponectin in insulin resistance. *Clin Chim Acta* 417:80–84.

Zakharov D, Lapish C, Gutkin B, Kuznetsov A (2016) Synergy of AMPA and NMDA receptor currents in dopaminergic neurons: a modeling study. *Front Comput Neurosci* 10:48.

Zweifel LS, Parker JG, Lobb CJ, Rainwater A, Wall VZ, Fadok JP, Darvas M, Kim MJ, et al. (2009) Disruption of NMDAR-dependent burst firing by dopamine neurons provides selective assessment of phasic dopamine-dependent behavior. *Proc Natl Acad Sci U S A* 106:7281–7288.

(Received 28 January 2021, Accepted 5 May 2021)
(Available online 13 May 2021)